Resistance to biodeterioration of aluminium-rich binders in sewer network environment: Study of the possible bacteriostatic effect and role of phase reactivity

Amaury Buvignier, Cédric Patapy, Matthieu Peyre Lavigne, Etienne Paul, Alexandra Bertron

Resistance to biodeterioration of aluminium-rich binders in sewer network environment: study of the possible bacteriostatic effect and role of phase reactivity

Amaury Buvignier[a,b], Cédric Patapy[b], Matthieu Peyre Lavigne[a], Etienne Paul[a], Alexandra Bertron[b,*]

a LISBP, Université de Toulouse, CNRS, INRA, INSA, 135 Avenue de Rangueil, 31077 Toulouse, France.

b LMDC, Université de Toulouse, INSA, UPS, 135 Avenue de Rangueil, 31077 Toulouse, France

* Corresponding author: bertron@insa-toulouse.fr

Keywords: Durability (C); Calcium aluminate cement (D); Portland cement (D); Granulated Blast-Furnace Slag (D); Waste management (E)

Abstract

This paper aims to better understand the mechanisms explaining the superior resistance of calcium aluminate cement (CAC) materials compared to Portland cement (PC) based materials in sewer networks. The bacteriostatic effect of CAC materials on Sulfur Oxidising Bacteria (SOB) is often argued in the literature as a possible mechanism explaining their better resistance. Reactor tests conducted on SOB demonstrated their ability to acclimatise to high aluminium contents. More generally, using a laboratory biodeterioration protocol reproducing aggressive conditions, the nature of the material (CAC or PC with different slag contents) did not significantly affect the SOB selection. Moreover the CAC materials seemed to favour the development of a higher SOB activity (and so acid production) than PC-based systems, leading to more aggressive conditions. Finally, the resistance of

CAC materials to biodeterioration appeared to be mainly linked to the intrinsic resistance of phases initially present or precipitated during the deterioration process.

1. Introduction

The local biological production of H_2S released in the aerial part of sewer networks and its biological oxidation into H_2SO_4 are partly the cause of deterioration of their cementitious materials [1,2]. In very aggressive conditions (humidity, temperature, hydraulic constants, H_2S levels etc.) and with a conventional concrete formulation, the lifespan of concrete structures may be reduced to below 10 years [3,4]. Such biodeterioration leads to major problems in wastewater collection and treatment, implying significant rehabilitation costs [5,6].

The biodeterioration of concrete in sewer networks is the result of a series of complex biological and chemical reactions: (i) In stagnant zones (in organic-rich wastewater), sulfate-reducing bacteria (SRB) reduce sulfate into H_2S in anaerobic and nitrate depletion conditions [7]. This compound degases into the headspace of the networks and condenses on the upper part of the cementitious coating by absorption and diffusion. The chemical reactions of the H_2S - and the CO_2 – on a hardened concrete (with surface pH ranging from 11 to 13.5 [2]) induce a decrease in the pH at the material surface to around 9 [8]. The abiotic reactions of H_2S with the cementitious matrix produce several sulfur compounds with different degrees of oxidation [9]. These precursors (thiosulfate (S_2O_3), elemental sulfur (S^0), etc.) are sources of electrons for bacterial development. The pH conditions and the sulfur compounds create a suitable environment for sulfur-oxidising bacteria (SOB) to develop. With the transformation by SOB of the reduced sulfur into H^+ and SO_4^{2-} as final oxidation products [2,10], successive populations of SOB develop during the pH decrease. The first bacterial succession concerns the neutrophilic sulfur-oxidising bacteria (NSOB) which results in a progressive pH decrease from 9 to 4 [2,11]. However, starting from pH 4, the environmental conditions are no longer suitable for the growth of NSOB and, hence, acidophilic sulfur-oxidising bacteria (ASOB) – the second bacterial succession – develop [2,9,12]. The development of ASOB is considered as the main active

stage of biodeterioration due to the high production of sulfuric acid [2,9,13]. In this range of pH *Acidithiobacillus Thiooxidans* is reported as the predominant aerobic bacterial species responsible for the acidification [3,13]. The attack of the cementitious material by the aggressive agent produced by the microbial activity is usually called biogenic acid attack. Grengg et al. [14] showed the presence of bacteria deep inside the deteriorated area of concrete exposed to sewer conditions in situ. Moreover these authors demonstrate the role in the biodeterioration process of *Acidithiobacillus ferrooxidans* using Fe as an energy source in anaerobic areas far from the surface of the concrete.

The deterioration of the cementitious matrix by biogenic acid is a dual attack by acid (H^+) and by sulfate (SO_4^{2-}). Decalcification and dissolution of the main calcium-based phases (portlandite (noted CH) and C-A-S-H for PC-based material and $3CaO.Al_2O_3.6H_2O$ (katoite or C_3AH_6 in cementitious notation) for CAC-based material lead to the formation of silica or alumino-silica rich deteriorated areas on the upper part of the material in contact with the biofilm [2,15]. The so called siliceous gel observed for PC systems is mainly amorphous and the alumina gel for CAC is mainly composed of $Al(OH)_3$ phases (noted AH_3 using cementitious notations)[16]. On the other hand, the diffusion of sulfur compounds in the porosity of the cement matrix and their reaction with hydrated phases induces the precipitation of sulfate based phases (often identified as gypsum and ettringite) [17,18].

The combination of these phenomena is commonly called Microbial Induced Concrete Corrosion (MICC) even though the term “corrosion” might be reconsidered in a biogenic acid attack. The biodeterioration of the cementitious materials combines biological, physical and chemical reactions and occurs in a complex system associating microorganisms, the material and the surrounding environment (sulfur substrate level, temperature, humidity, hydraulic constant, etc.). [4,17].

Therefore, accelerated biodeterioration protocols are needed in order to obtain data in several months and to dissociate the different key parameters of the resistance of materials to biogenic acid attack. [19,20], [21,22], A test was developed at the University of Toulouse (called BAC test for Biogenic Acid Concrete test) [23,24] for this purpose, which uses the development of a biofilm on the surface of a cementitious material fed by trickling tetrathionate solution over it. The use of a liquid sulfur substrate instead of H_2S – often used in laboratory tests – allows the feeding and the leaching solution

to be analysed and thus the biological transformation of the sulfur and the progressive leaching of the cementitious matrix to be monitored through mass balance [25]. In the BAC test, the inoculum is composed of sludge from a waste water treatment plant. The use of a diversified inoculum takes the biodiversity into account while selecting the sulfur-oxidising function.

Calcium Aluminate Cement (CAC) based materials have demonstrated a higher resistance to a biogenic acid attack than PC-based materials, in both on-site and laboratory conditions [15,17,25,26]. A range of hypotheses have been emitted by different authors to account for this better resistance. They can be divided into two categories: the physicochemical resistance of the material, i.e. its capacity to resist the chemical attack because of the chemical and physical properties of the original and newly formed phases, and the biological resistance, i.e. the ability of the material to influence or hinder the biological activity, leading to less severe attack on the material. In the first category, many authors attribute the higher durability of CAC-based materials to: (i) the higher neutralisation capacity of these materials compared to PC-based materials, which would neutralise a larger amount of biogenic acid, (ii) the greater stability of original hydrated phases (including C_3AH_6 and/or phases newly formed through acid attack (AH_3), compared to calcium silicate phases (CH, C-A-S-H and silica gel), and (iii) the low porosity of AH_3 gel of biodeteriorated CAC matrix, which would slow down transport processes [15,19,26–28]. Concerning the biological resistance, the bacteriostatic effect of aluminium is often mentioned. It is thought that the release of Al^{3+} by the CAC matrix inhibits the SOB activity, leading to a decrease in biogenic sulfuric acid production, and that the neutralisation capacity of CAC mortar would limit the SOB growth by depriving them of their ideal growth conditions and so decreasing the biogenic sulfuric acid production [12,17,19,26,29]. However, no real consensus and no direct evidence or robust demonstration of the validity of the different hypotheses are to be found in the literature so far.

The aim of the present work was to better understand the mechanisms explaining the better resistance of CAC materials compared to PC-based materials in sewer network conditions, and to assess each previous hypothesis. The possible bacteriostatic effect of aluminium was assessed by studying the influence of soluble aluminium on SOB activity in reactor conditions. Then, the influence of the

nature of the material (composition, neutralisation capacity, etc.) on the SOB biofilm settlement, development and activity during biodeterioration was examined using a laboratory test (BAC test). Finally, the influence of the chemical species produced by the biological activity on the material was studied, in order to understand the relationship between the physicochemical characteristics of a cementitious material (composition, porosity, etc.) and its resistance to deterioration.

To understand the influence of physicochemical characteristics of cementitious binders and, in particular, the role of aluminium on the biotic activity, materials containing various aluminium contents and with different aluminium mineralogical forms were selected. PC-based materials with different substitution rates of ground granulated blast-furnace slag (GGBS) (from 0 to 95%) and CAC-based materials with two different types of thermal curing were cast.

2. Materials and testing procedure

2.1 Preparation and characterisation of cement pastes

Cement paste specimens were made with a white PC, CEM I 52.5N CE CP2 (Lafargeholcim, Le Teil, France) substituted with different amounts of commercial superfine GGBS (Ecocem Ltd, Ireland) from 0 wt.% to 95 wt.%. CAC (Secar 51, Kerneos, France) based samples were also cast (Tables 1 and 2). The chemical compositions in Table 1 were obtained by XRF analysis. The Blaine surface was evaluated with the method described in the standard NF EN 196-6. Phase quantification data in Table 2 were obtained by quantitative XRD with Rietveld refinement. A white PC was chosen in this study (i) to limit the presence of iron, which can influence the development of some acidophilic bacteria and.

Water intrusion porosimetry was performed on cement samples before exposure to the BAC Test. The samples were kept in a vacuum for 4 hours to remove any air entrapped in pores. Afterwards, the pores of the samples were filled with water under vacuum conditions for 24 hours. The samples were then removed from the water and hydrostatically weighed before being dried at 105 °C. The samples were

130 weighed daily until the difference between two successive weighings, 24 hours apart, was less than
131 0.05%. The porosity and the apparent density were then calculated [30].

132

133 **Table 1. Oxide composition of PC, GGBS and CAC**

	PC	GGBS	CAC
CaO	66.6	43.3	37.9
SiO_2	22.0	37.1	5.1
Al_2O_3	2.3	11.1	52.1
MgO	0.5	6.5	0.3
Fe_2O_3	0.3	0.6	1.6
TiO_2	<0.1	0.5	2.1
K_2O	0.5	0.2	0.4
SO_3	3.4	0.2	<0.1
other oxides	4.8	0.5	0.5
loss on ignition	3.8	<1.5	/
Blaine	4250	7500	3870

134

135 **Table 2. Mineralogical composition of PC and CAC.**

Phases:	**C_3S**	**C_2S**	**C_3A**	**C_4AF**	**$CaSO_4.0.5H_2O$**	**Calcite**
PC (wt.%)	58	28	6	1	2.5	5
Phases:	**CA**	**$C_{12}A_7$**	**C_2AS**	**C_2S**	**Q-phase**	**Perovskite**
CAC (wt.%)	67.3	0.4	20.1	5.0	2.4	4.2

136

137 Cement paste specimens were prepared with a water/binder (w/b) ratio of 0.4 for PC-GGBS binders
138 and 0.3 for CAC binders. In EN-196-1 the w/b ratio is 0.5 for PC-based mortar, and in EN-14647 the
139 w/b ratio is 0.4 for CAC mortar. Specimens were cast in rectangular plastic moulds with dimensions

5*4*1 cm^3 and demoulded after 24 hours of hydration. PC-based specimens were stored at 20 °C in sealed plastic bags for 90 days. Two types of thermal curing were used for CAC specimens in order to evaluate the influence of conversion of metastable hydrates on the resistance of the material to biogenic acid attack. After casting, a first series of CAC was cured for 16 hours at 70 °C (98% RH) followed by 8 hours at 20 °C (98% RH) to ensure that conversion took place (the specimens were called CAC-70°C). A second series of CAC was not exposed to any thermal curing and was kept at 20 °C (called CAC-20°C). CAC specimens were stored at 20 °C in sealed plastic bags for 90 days.

After curing, the cast face located on the bottom of the mould (5*4 cm^2) was selected for exposure to the BAC-test whereas the other faces were protected from acid attack with a special epoxy resin coating (EUROKOTE 48-20 from BS COATING). The longitudinal edges (each 5 cm long and 3 mm thick) of the uncoated and further exposed cast surface were also coated with the epoxy in order to guide the liquid dripping on the sample during the BAC test. These guides were later used as a reference for measuring depth of deterioration.

The mineralogical features of the OPC-GGBS hydrated binders (Figure 1) at 90 days before exposure to the BAC-test were determined by mass balance based on the method described by Yu et al. [31].

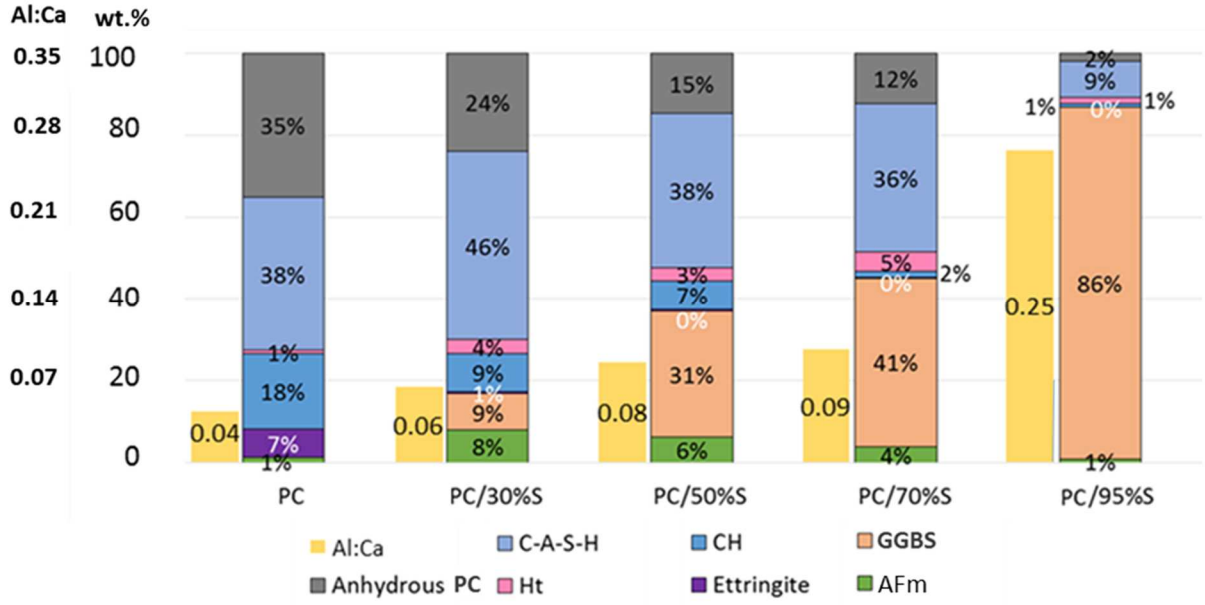

Figure 1. Phase assemblage estimation of PC with 0%, 30%, 50%, 70% and 95% of GGBS sample after 90 days' hydration. On the left, Al:Ca molar ratio in the binders.

Mass-balance calculations were carried out to quantify approximately the amount of C-S-H and poorly-crystalline hydrates such as AFm. Actually, a direct quantification of these phases by TGA, NMR (^{27}Al for example), SEM or XRD coupled with Rietveld refinement is very difficult, if impossible.

The amount of anhydrous clinker and that of GGBS were measured by SEM-based methods (on the basis of Mouret et al. and Kocaba et al. approaches [32,33]). Quantitative analysis of backscattered electron images with image analysis (BSE and IA) coupled with EDX (i.e., energy dispersive x-ray spectroscopy) were done to quantify the residual anhydrous phases. Mg-EDS mapping were used to separate CH areas and GGBS grains showing closed grey levels. Figure 2 illustrates the measurement of the degree of GGBS reaction using SEM-EDX methods.

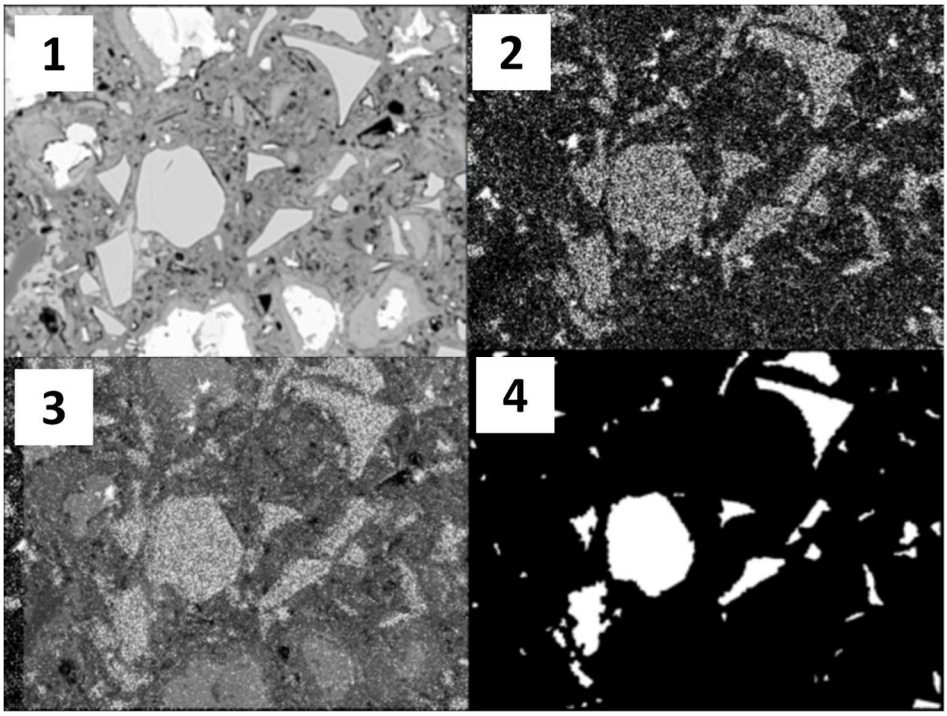

Figure 2. The steps applied in measurement of the degree of slag reaction using SEM-EDX methods: (1) SEM image, (2) Mg-EDS Mapping, (3) Superimposition of BSE and EDS images and (4) Identification of the GGBS particulates (unreacted).

As such, assuming standard stereological correlations for randomly distributed microstructures, the residual anhydrous clinker and GGBS can be determined. Thirty BSE images were acquired on plane polished paste sections using a JEOL JSM 6380 LV scanning electron microscope (SEM) at a magnification of 900x. The total amount of Ca, Si, Al, Mg, S and C released during the hydration was calculated, knowing the chemical composition of PC and GGBS. All the Mg was considered included in hydrotalcite ($Mg_4Al_2O_7 \cdot 10H_2O$), and Al relative to the chemical formula was substracted. All the Si was assumed to be incorporated in C-S-H, and Ca, Al, and S were subtracted based on the Ca/Si, Al/Ca, and S/Si ratios in the C-S-H measured by SEM-EDS pointing. The ettringite was quantified by

XRD-Rietveld, and Ca, Al and S were subtracted. The remaining S was considered included in monosulfate, subtracting Ca and Al. Finally, the remaining Ca was attributed to CH.

One of the main error of the mass-balance calculation is the evaluation of the quantity of monosulfate, because it is calculated from the amount of sulfate after assignment to C-S-H and to ettringite. In this study, the ettringite peak for OPC-GGBS systems is very low and in the error range of the method (no more than 1 wt.%). The accuracy of mass balance calculations of hydrates is then likely questionable. But this simplified mass balance calculation allows addressing the main correlations between major changes in phase assemblage and resistance to biodeterioration.

The relative proportion of C-A-S-H decreased and the Ca:Al ratio increased with higher substitution levels of GGBS. Hydrotalcite (Ht) and monosulfoaluminate (AFm) were present in small proportions. The ettringite content was very low in GGBS blended systems, probably due to a sulfate deficit. The proportion of unreacted GGBS was high and increased with higher substitution levels.

XRD analysis have been done on solid samples of CAC 20°C and CAC 70°C before exposure to the biodeterioration test. The qualitative XRD analyses revealed the presence of C_3AH_6 and AH_3 for CAC 70°C, and presence of AH_3, $CaO.Al_2O_3.10.(H_2O)$ (noted CAH_{10}) (with traces of C_3AH_6 for the system CAC 20°C). No $2CaO.Al_2O_3.8(H_2O)$ (noted C_2AH_8) was spotted in neither sample. A simplified phase assemblage has been calculated for both CAC 20°C and CAC 70°C systems. The CA phase is the major phase in CAC cements and the most reactive one (with $C_{12}A_7$ which is present in a very low content, i.e. 0.4 wt.%). In the proposed phase assemblage, the CA phase is considered as the only anhydrous phase reacting during hydration. The contents of the other anhydrous phases of the CAC (C_2AS, C_2S, Q-phase, perovskite) are supposed to be constant between 0 and 90 days. The residual quantity of anhydrous CA grains was determined by SEM image analysis based on BSE grey levels according to the same method as the quantification of anhydrous PC. Gosselin has already shown the ability of satisfactorily isolating the CA phase contribution on the grey-level histogram in SEM-BSE mode and the ability to accurately quantify this anhydrous phase by this method [34]. The residual content of CA was 0 wt.% and 29 wt.% for the CAC 70°C and CAC 20°C systems, respectively. The CAC 70°C system was thus significantly more hydrated than the CAC 20°C one. Equations Eq. 1 and Eq. 2 were used for mass balance calculations of hydrate formation for CAC 70°C and CAC 20°C, respectively [34]. These results are in accordance with experimental results of the literature showing that a 20°C curing of CAC cements favors the formation of CAH_{10} which is potentially metastable whereas the 70°C curing enhances the production of C_3AH_6 and AH_3 through the so-called process "conversion phenomena".

$$3CA + 12H \rightarrow C_3AH_6 + 2AH_3 \quad \text{Eq. 1}$$

$$CA + 10H \rightarrow CAH_{10} \quad \text{Eq. 2}$$

The results of the mass balance calculation for the CAC 70°C and the CAC-20°C system are detailed in Figure 3.

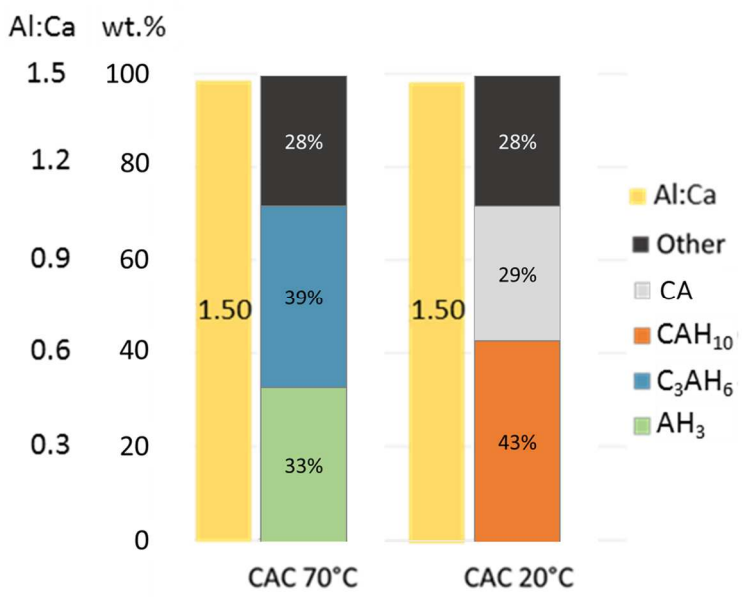

Figure 3. Phase assemblage of CAC-20°C and CAC-70°C. On the left, Al:Ca molar ratio in the binders.

AH_3 is only present in CAC-70°C, in a comparable mass proportion to C_3AH_6 (respectively 33 and 39 wt. %). The main hydrated phase of the CAC-20°C system is CAH_{10}

2.2.2 Hydroxide potential of materials tested

One of the literature hypotheses explaining the better resistance of CAC-based material is the higher neutralisation capacity of CAC binders [15,19,27]. During the biodeterioration of the material, oxides present in the matrix are dissolved, which induces the release of hydroxide. The theoretical amount of hydroxides dissolvable in each tested material was calculated. This "hydroxide potential" depends only on the chemical composition of the material and not on the phase assemblage. If all oxides in a

material are dissolved, the hydroxide potential corresponds to the molar amount of OH^- that can be released and is named PtOH (total OH^-potential) in what follows.

In the first stage of acid attack, and biogenic acid attack in particular, the deterioration process corresponds to the decalcification of the material, with dissolution of CH and C-A-S-H for PC-based material and decalcification of C_3AH_6 (and CAH_{10}) into AH_3 for CAC-based material [15,24,35]. An intermediate OH- potential, PiOH, corresponding to the first stage of the deterioration of a material, i.e. the release of calcium (calculated only from the initial calcium oxide composition obtained by XRF on anhydrous samples) from the decalcification of CH, C-A-S-H, C_3AH_6, and CAH_{10}, can thus be calculated. The PiOH corresponds to the neutralisation capacity when pH starts to decrease (formation of new deterioration products) until all the initial phases have been dissolved. The dissolution reactions used for this study are reported in Table 3. Potassium, sulfur and titanium oxides were not taken into account because of their low contribution to the potential. It can be noted that SiO_2 did not participate in the hydroxide potential calculation.

Table 3. Dissolution reactions taken into account in the calculation of PtOH and PiOH.

Oxide	Dissolution reaction
CaO	$CaO + H_2O \rightarrow Ca^{2+} + 2OH^-$
SiO_2	$SiO_2 + 2H_2O \rightarrow H_4SiO_4$
Al_2O_3	$Al_2O_3 + 3H_2O \rightarrow 2Al^{3+} + 6OH^-$
MgO	$MgO + H_2O \rightarrow Mg^{2+} + 2OH^-$
Fe_2O_3	$Fe_2O_3 + 3H_2O \rightarrow 2Fe^{3+} + 6OH^-$

The OH^- potential was calculated by summing the moles of OH^- per gram of material, reported in mole of OH^- per volume of material (taking the density and porosity of each material into account [36]). It was then converted into a molar amount of OH^- for a given surface by multiplying by an arbitrary thickness of the material (1 cm).

Figure 4 shows a) the PtOH and the PiOH of the different cement pastes tested and b) a comparison with the neutralisation capacity calculated by Letourneux and Scrivener [37].

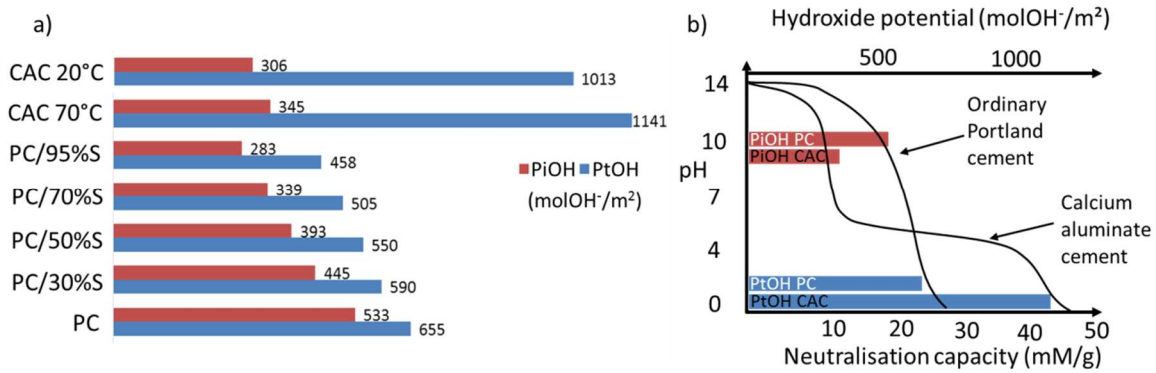

Figure 4. a) Intermediate OH^- potential (PiOH) and total OH^- potential (PtOH) for PC-based material substituted with 0 to 95% of GGBS and for CAC-based material (in $molOH^-/m^2$). b) Neutralisation capacity and hydroxide potential of CAC and PC (adapted from Letourneux and Scrivener [37]).

With increasing GGBS contents, the PiOH and PtOH of PC-based material decreased because of the lower amount of CaO in GGBS than in PC. The intermediate potential was higher for PC-GGBS pastes than for CAC pastes because of the higher CaO content. However, the PtOH of CAC-based material was the highest. The large discrepancy between PiOH and PtOH for CAC matrix corresponds to the dissolution of AH_3, the product of CAC phase dissolutions because of acid attack. When pH decreases to below 4, AH_3 starts dissolving and it releases 3 moles of OH- per mole of the molecule, which explains the large increase of hydroxide potential at this pH. These results are in accordance with the neutralisation capacity calculated by Letourneux and Scrivener [37] as represented in Figure 4b).

2.4 Experimental set-up for cement paste biodeterioration using biofilm development

A laboratory test developed at the University of Toulouse, the BAC test, was used to expose the cementitious specimens to sewer-like environments in accelerated conditions. This test set-up was

designed to ensure the development of sulfur-oxidising microorganisms on the surface of a material, evolving over time and depending on the physicochemical characteristics of the material tested [23]. For this purpose, a mineral solution of selected concentrations of soluble reduced sulfur was trickled over the surface of a material previously inoculated by a microbial consortium of NSOB and ASOB selected from a waste water treatment plant sludge (Toulouse, France). The mineral solution contained tetrathionate ($S_4O_6^{2-}$, reduced sulfur intermediate compound in the oxidative chain of sulfur) allowing the selection of a sulfur-oxidising activity in the biofilm, and leading to the production of acid and sulfate in contact with the surface of the material [24,25]. The test was monitored by the quantification of biogenic sulfate (and consequently acid) produced, and released calcium and aluminium in the leaching solution collected downstream of the specimen. The reproducibility and representativeness of the test has been demonstrated [24,25].

An optimised configuration of the test previously developed by Peyre Lavigne et al. [23] was used (Figure 5). Cement paste was preferred rather than mortar lining to focus on the reactivity of the cementitious phases of the material and to facilitate SEM and XRD analyses. Specimens were tilted by less than 5° in order to impose high retention time and to promote chemical equilibrium between the bulk, the biofilm and the cementitious material. The exposure time was slightly longer (4.3 months or 133 days) in this study than in previous ones (3.7 months in [23]) because of the small amount of microorganisms inoculated on the material and the lower sulfurous substrate flow (~5.81 molS/m²/d in this study vs. max. 7.44 molS/m²/d in [23]), but the acid flow in contact with the material was three times higher (~250 $molH^+/m^2$ on average in this study) inducing more calcium leaching per square meter.

Downstream of each exposed specimen, the solution was collected for 1 h twice a week (~20 mL collected) in order to monitor the flow rates, pH (analysed with Schott sensor) and concentrations of sulfate produced, and calcium and aluminium leached (analysed by ion chromatography DX320-Dionex Thermofisher) (4).

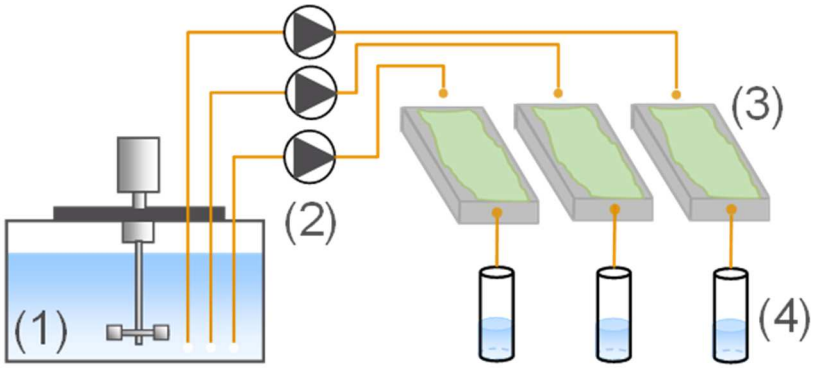

Figure 5. Schematic diagram of the BAC test.

2.5 Experimental set up for sulfur-oxidising activity measurement

Sulfur-oxidising microorganisms grown in different conditions were exposed to various concentrations of soluble aluminium in reactors in order to evaluate a possible bacteriostatic effect of this ion. For the experiment in slighty acidic conditions (pH ~4), biofilms from WWS were developed on CAC pastes (CAC condition) and on an "inert" plastic material (inert condition) using the BAC test in the conditions described in section 2.4, for 2 months. The biofilms were removed using a water flow and then mixed in order to disperse bacteria, and finally introduced into an open jacketed reactor of 300 mL. These two conditions were chosen in order to look at the influence of the nature of the material environment on SOB possible selection and thus on different SOB populations. For the experiment in a highly acid environment (pH ~2), a controlled 1.6 L open reactor was seeded with active sludge from the wastewater treatment plant of Toulouse (France) and fed with nutritive solution. The sulfur-oxidising activities were studied in gas open batch reactors (thermostated at 20 °C) using respirometry (with online measurement of dissolved O_2 concentration (Hamilton sensor), pH (Schott sensor), and temperature (Hamilton sensor)) [38]. Aeration and measurement of oxygen uptake rates (OUR) were managed by sequentially bubbling pressurised air into the reactor. The aeration provided the O_2 and the CO_2 necessary for the growth of chemolithotrophic bacteria as SOB. The feeding consisted of successive pulses of a 0.2 M concentrated potassium tetrathionate solution (P2926-Aldrich).

For the experiments in a slightly acid environment, the pH was buffered at 4 by a CO_2 enrichment of pressurised air (~10%). For the experiment in the highly acid environment, the pH was not controlled, so a reference culture was operated in parallel.

Three different levels of aluminium concentration (0 mM, 50 mM and ~100 mM) were used in this study. Aluminium was added using $AlCl_3$ in order to keep the ionic strength modification to a minimum with the addition of inhibitory compound. During the biodeterioration of CAC and PC mortar using the BAC test (reproducing an accelerated aggressive deterioration), Peyre Lavigne et al. [25] measured a concentration of 0.5 mM of Al^{3+}. Herisson et al. [26] measured total aluminium concentration of condensed water in a PVC tube planted in CAC concrete exposed to a sewer network. They obtained a concentration of Al^{3+} of 125 mM. The range of concentration tested corresponds to concentrations that are possible in situ.

The activity was evaluated by measuring the bacterial yield and evaluating the maximum specific growth rate (μ_{max}) during a growth with a minimum of a doubling of the SOB population. The bacterial yield, Yo/s ($molO_2/molS_4O_6^{2-}$), was measured for every pulse of substrate by dividing the quantity of dioxygen consumed by the quantity of tetrathionate consumed. The μ_{max} was obtained by fitting a model developed on AQUASIM with the experimental OUR using the following equation (Eq. 3).

$$OUR = A * \exp(\mu_{max} * t) \quad \textbf{Eq. 3}$$

where OUR is the oxygen uptake rate in $mgO_2/L/h$, A is a constant in $mgO_2/L/h$, μ_{max} is the maximum specific growth rate in h^{-1}, and t is the time in h.

The model was verified twice: with successive growth in pulses of sulfur and in constant excess of sulfur. The details of the device are reported in [36,39]. The accuracy on the μ_{max} and on the bacterial yield data were ± 0.003 h^{-1} and ± 0.11 $molO_2/molS_4O_6^{2-}$, respectively, representing relative errors of ~6% and ~3%, respectively. To evaluate the effect of aluminium chloride on the bacteria, the μ_{max} and the Yo/s with and without the compound were compared. The adaptation of bacteria to the compound was evaluated by successive growth over several days for a constant aluminium concentration.

341

342 **2.6 Analyses of cement pastes exposed to SOB activity in the BAC test**

343 At the end of the exposure period (4.3 months) of the cementitious specimens to the BAC test, 1 cm
344 thick cement paste slices were cut along the cross section of each specimen, i.e. perpendicularly to
345 their surface in contact with the biofilm (or interface). The chemical and mineralogical composition of
346 the specimens was analysed as a function of the distance to the interface using scanning electron
347 microscopy (SEM coupled with energy dispersive spectrometry (EDS) and X-ray diffraction (XRD).

348 For SEM analyses, the slices were embedded in an epoxy resin (Mecaprex MA2 from Presi) in small
349 moulds prior to polishing. The polishing was performed using a series of three silicon carbide
350 polishing disks: P800-22µm, P1200-15µm, and P4000-5µm using the protocol described in [40]. After
351 polishing, the sections were coated with carbon. Alteration patterns were observed with SEM (JEOL
352 JSM-6380LV) in BSE mode. One control specimen was also analysed 90 days after casting for
353 comparison. Chemical analyses were carried out using EDS (BRUCKER XFLASH 6l30).

354 XRD analyses (D8 ADVANCE Brucker diffractometer - CuK_α radiation (λ=1.54Å)) were performed
355 on bulk samples, with a progressive abrasion of the surface in order to characterise the different depths
356 of deterioration using the protocol described in [41]. The acquisition was achieved with a step size of
357 0.02°, 0.25 sec per step, in the 2 theta range of 4°-24°. The mineralogy was identified with the help of
358 the software EVA. XRD analyses of the biodeteriorated materials were carried at different depths in
359 the sample i.e. 1) on the top of the deteriorated surface, 2) at a few hundred micrometres below the top
360 surface and 3) in the sound area of the sample (at about 1.5 cm deep). The specimens were abraded
361 with SiC abrasive paper (P800-22µm) between two successive analyses. The different depths were
362 controlled by measurements with a calliper.

363 **2.7 Biofilm preparation for scanning electron microscopy observation**

364 A small prism of cement paste (3 mm * 4 mm * 2 mm) was positioned on the surface of each
365 specimen tested during exposure to the BAC test. With the development of biofilm on the surface, the
366 small piece of material was also covered by biofilm and deteriorated. After 133 days of exposure,

these pieces of material covered by biofilm were collected and prepared for observation. In order to observe the biofilm morphology, the water present in bacterial cells was removed without destroying the integrity of the cell walls. The protocol consisted of aldehydic gelification and dehydration. Samples were immersed in paraformaldehyde solution (4%) for 3 hours and washed for 8 times 10 minutes in a saline phosphate buffer. Samples were then washed in successive baths of water/ethanol solution with increasing ethanol concentrations (15 minutes in 50% ethanol, 15 minutes in 75% ethanol and 30 minutes in 96% ethanol). Samples were then dried for 3 hours at 30 °C and fixed on specimen holders 0.5 cm in diameter, tilted at 45°. Samples were then covered by a thin layer of gold. Observations were made using SEM-FEG in SE mode (JSM 7100F TTLS). The bacterial structure seemed not to be altered by drying during SEM observations (walls of bacteria were not damaged).

3. Results

The influence of the material on the biofilm will be presented: (i) the influence of soluble Al^{3+} on SOB in reactor, to evaluate the bacteriostatic effect and (ii) the effect of the material on the biofilm morphology, composition and metabolism. Then, the effect of the biofilm on the material will be presented: (iii) the analyses of the leaching solution during the biodeterioration, providing leaching kinetics, and the observation of deterioration patterns together with deteriorated depths.

3.1 Influence of soluble Al^{3+} on SOB

The maximal specific growth rate (μ_{max}), and the oxidation yield ($Y_{O/S}$) were measured. Preliminary tests were performed up to 30 mM but they did not reveal any rapid influence of the injection of aluminium on the SOB oxygen uptake rate, so they are not presented here.

Figure 6 represents the evolution of μ_{max} measured without addition of soluble aluminium (0 mM, time t0), after a first injection of Al^{3+} = 50 mM at time t1, and after a second injection leading to a final concentration of Al^{3+} = 100 mM at time t2. Maximum specific growth rate was measured immediately

after each injection of soluble aluminium, and 24h after the first addition of Al^{3+} (50 mM, t1+24h). Values of t1 and t2 depended, among other parameters, on the bacterial growth rate and on the time between two successive pulses of tetrathionate.

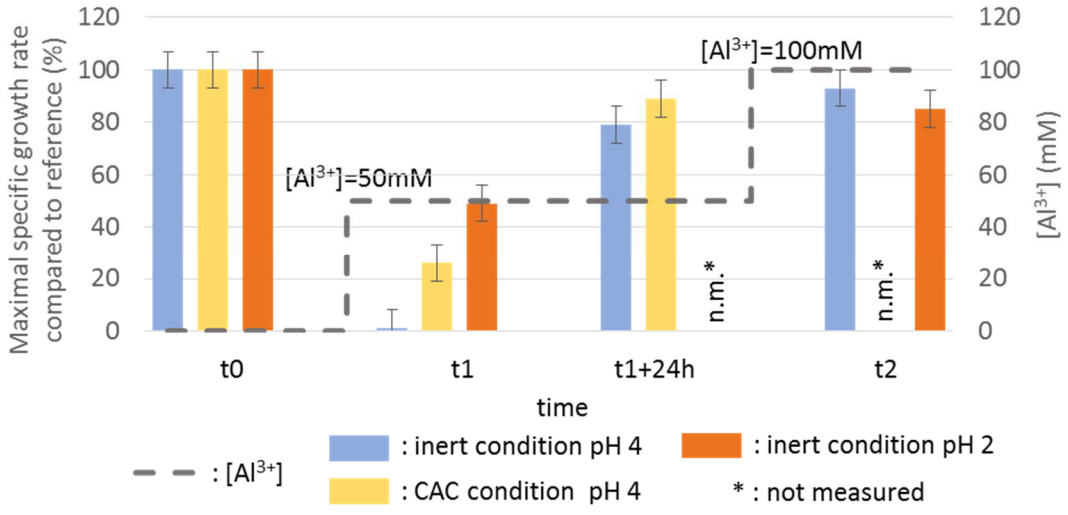

Figure 6. Maximal specific growth rate for successive Al^{3+} additions, for different growth conditions. *not measured.

Before any Al^{3+} addition to the medium (t0), the maximal specific growth rate was measured and was then used to standardise further measurements. At t0, μ_{max} was thus equal to 100%. SOB developed in all further growth conditions suffered a temporary decrease in μ_{max} with injection of 50 mM of Al^{3+} (t1). Figure 6 shows that, after 24 hours of acclimation to the aluminium injection (t1+24h), SOB were no longer significantly affected by soluble aluminium in terms of maximum specific growth rate. This was due to the acclimation of SOB to the chemical conditions. After the second injection of $AlCl_3$ (total concentration of 100 mM of Al^{3+}) at time t2, the μ_{max} was not significantly different from the control growth. A high level of aluminium no longer modified the activity of SOB. It can be noted that, for each injection of $AlCl_3$, the $Y_{O/S}$ (not shown here)[36,39] increased significantly (by about 10%), meaning that the bacteria needed energy to adapt to their environment. After acclimation to the injection of aluminium, SOB recovered the initial oxidation yield value and they no longer overconsumed energy to survive.

411 The growth conditions of the biofilms used in the experiment significantly impacted μ_{max}, essentially
412 after the first injection of Al^{3+}=50 mM (time t1), whereas no significant effect was observed for other
413 measurements. For SOB developed at pH=4 in inert conditions, bacteria were so disturbed right after
414 the 1st injection (t1) that no μ_{max} could be measured. For SOB developed on the CAC samples,
415 standardised μ_{max} was 23%, i.e. these SOB resisted better than those developed in inert conditions. The
416 pre-acclimation of SOB to the aluminium and high salt concentration due to the contact between the
417 biofilm and the CAC material induced a possible selection of SOB resistant to this environment. The
418 pH conditions of the biofilm growth were also probably responsible for a selection of resistant
419 microorganisms. Actually, SOB developed at pH=2 in inert conditions showed a lower decrease in
420 μ_{max} after injection of 50 mM of Al^{3+} than those developed on the same support at pH =4. It can be
421 noted that the form of aluminium at pH<4 was more than 95% free Al^{3+} [42]. Therefore activity
422 analyses for both pH levels were performed with the same inhibitory compound.

423 The experiment was also run at pH=2 using NaCl instead of $AlCl_3$ with the same ionic force (data not
424 shown)[36,39]. The modification of osmotic pressure induced in the solution by the modification of
425 the ionic strength when NaCl was added provoked a temporary decrease of μ_{max}. So, the very short
426 term effect of $AlCl_3$ can be attributed to a modification of the osmotic pressure induced by a sudden
427 modification in ionic strength, rather than by a specific effect of aluminium.

428 In conclusion, whatever the growth conditions, the experiment demonstrated an adaptation of
429 microorganisms to their environment. Even though a short term effect was observed, soluble
430 aluminium did not seem to have a significant effect on SOB activity after their acclimation.

431

432 **3.2 Influence of the nature of the material on the microbial development**

433

434 **3.2.1 Influence of the neutralisation capacity of the material on the pH evolution and sulfate**
435 **production (biological activity)**

The influence of the nature of the material on the SOB development was studied. The aim was to understand whether, as the literature assumes, the better resistance of CAC-based material could be explained by an effect of the solid material surface on SOB activity in the form of a biofilm i.e. on biogenic sulfuric acid production, for a given SOB inoculum.

PC-based pastes with substitutions of 0 w.t.%, 30 w.t.%, 50 w.t.%, 70 w.t.%, and 95 w.t.% of GGBS and CAC-based pastes (with curing condition at 20°C or 70°C) were exposed to the BAC test for 133 days. The pH and the concentration of sulfate (expressing the sulfur-oxidising activity) of the leaching solutions trickled over the surface and collected downstream of each specimen (Figure 5) were monitored over time.

The evolution of pH with time is represented in Figure 7. The development of neutrophilic and then acidophilic SOB induced the production of sulfuric acid, decreasing the pH of the leaching solutions.

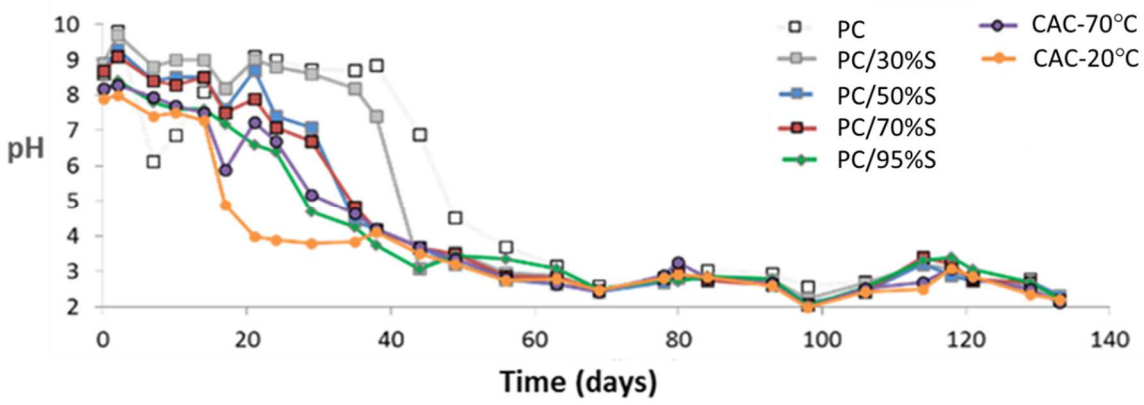

Figure 7. Evolution of pH of the leaching solution with time during BAC test biodeterioration

The evolution of the pH occurred in three phases. (i) One day after the beginning of the test, the pH was around 8 for CAC-based material and 8 to 10 for PC-based materials. Whatever the material composition, the pH remained high for at least 15 days. (ii) From day 15 and with a delay depending on the nature of the material, the pH decreased quickly due to the production of sulfuric acid by SOB. (iii) After the drop of the pH (ending at around 60 days for all the materials), leaching solutions were characterised by a relatively constant pH, around 2.5, until the end of the experiment (133 days).

Leaching solutions collected downstream of CAC-based materials showed an earlier decrease in pH than those of PC+GGBS based materials. With decreasing GGBS contents, the delay before the fall of pH increased. The 100% PC system showed the longest delay in pH fall (day 39).

Production of H^+ is associated with the production of sulfate and is directly linked to the SOB activity. Figure 8 shows the evolution of sulfate concentration in the leaching solution for each material tested. It can be noted that no significant sulfate production was observed before 60 days had elapsed, corresponding to the end of the pH drop for all the materials.

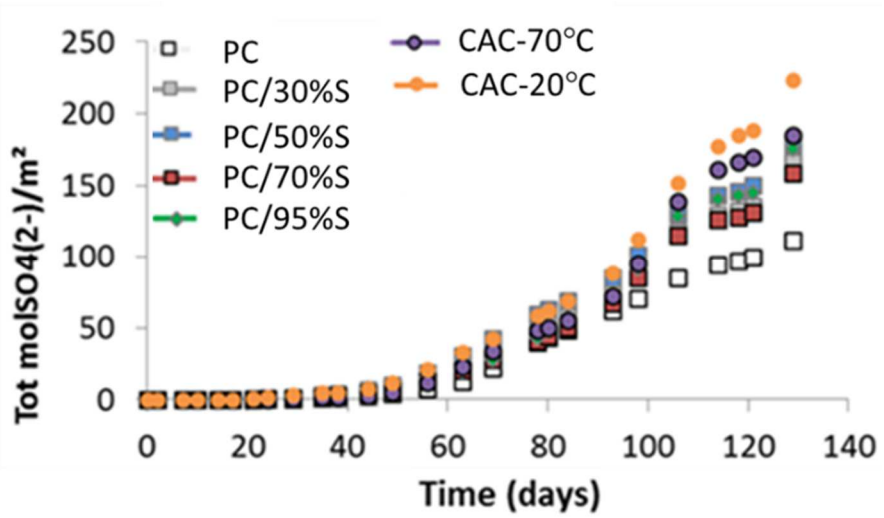

Figure 8. Evolution of sulfate concentration in leaching solution

At the early stage, before the fall in pH, sulfate production was low, corresponding to phase (i) of the pH evolution. After acidification and development of ASOB (corresponding to phase (iii) of pH evolution), the production of sulfate increased almost linearly with time.

CAC-based materials were characterised by the highest cumulative sulfate flow at any time. Despite the higher neutralisation capacity of CAC-based material, acidophilic SOB activity was also favoured on CAC materials, with no evidence of a bacteriostatic effect of the material on the biogenic sulfuric acid production, in the conditions of the test. (Cumulated final values: PC, 111 mol/m²; PC/30%S, 166 mol/m²; PC/50%S, 178 mol/m²; PC/70%S, 159 mol/m²; PC/95%S, 176 mol/m²; CAC-20°C, 224 mol/m²; CAC-70°C, 185 mol/m²)

475

476 **3.2.2 Effect on the selection of bacterial population**

477

478 In order to study the influence of the binder composition on the selection of bacteria on the surface of
479 the material, analyses of bacterial population were made on biofilm samples collected after 120 days
480 of exposure to the BAC test (data not shown) [36]. Similar biodiversity was observed on PC and CAC
481 materials with respectively 87% and 79% of *Acidithiobacillus thiooxidans* and around 7% of
482 *Thiomonas Intermedia*. These bacterial population analyses revealed no differences in the predominant
483 bacterial population according to the nature of the material.

484

485 **3.2.3 Observation of the biofilm morphology**

486

487 In order to study the influence of the material composition on the biofilm morphology, biofilm
488 developed on each of the materials tested using the BAC test were analysed as described in 2.7. After
489 133 days of exposure, the coupons supporting the biofilm were removed, and the biofilm was fixed,
490 dehydrated and then observed using SEM (Figure 9).

491

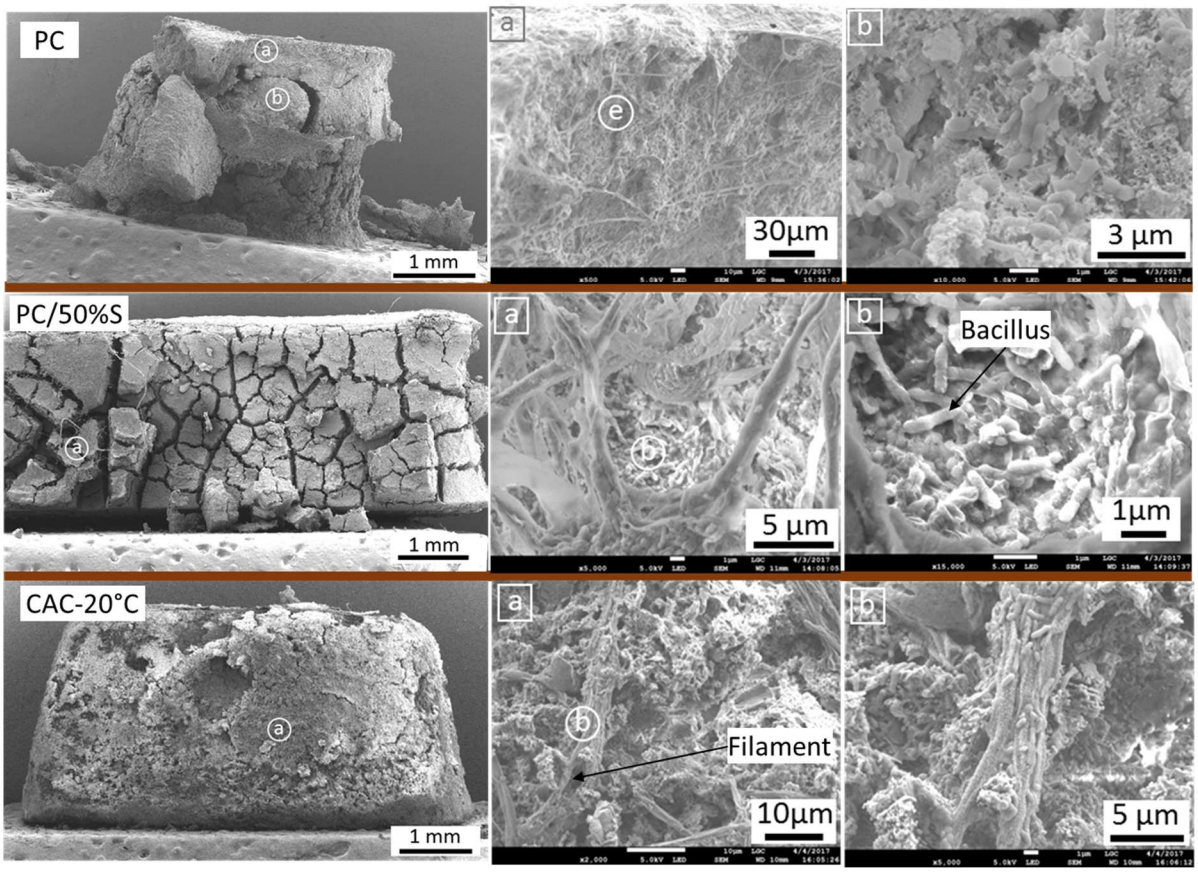

492

493 **Figure 9. SEM-FEG image in SE mode of biofilms developed on PC, PC/50%S and CAC-20°C cement paste after 133**
494 **days of exposure in the BAC test.**

495

496 The SEM images presented in Figure 9 reveal that biofilm morphology and covering were relatively
497 similar whatever the composition of the material. A large quantity of bacillus covered the surface of
498 the materials.. These bacteria were present in the cracks and under the freshly detached pieces of
499 materials. Filaments of ~1 µm diameter and of diameter >3µm were also present.

500

501 It could be observed that PCs were microcracked (Figure 9 left). Needle-shaped products crystallised
502 in microcracks may correspond to ettringite crystals, as suggested by EDS analyses (data not shown
503 [36]). The CAC surface remained more homogeneous with a smoother surface, which could indicate a
504 different behaviour toward the SOB attack from that of PC systems.

505

506 **3.3 Resistance of materials to biodeterioration: role of the chemical, mineralogical and**
507 **microstructural characteristics of the materials**

508

509 The following experiment dealt with the characterisation of the resistance to biodeterioration of the
510 materials tested using the BAC test. The evolution of chemical features of the leaching solution during
511 biodeterioration will be presented, followed by microstructural analysis of deteriorated materials.

512

513 **3.3.1 Calcium and aluminium concentration in leaching solution during biodeterioration**

514

515 During the exposure of the tested materials to the BAC test, the sulfuric acid produced by SOB
516 induced leaching and dissolution/precipitation of phases in the cement matrix. Calcium and aluminium
517 concentrations in the leaching solution were monitored to evaluate the kinetics of biodeterioration of
518 the different materials. To enable comparison of leaching among the different materials, the leached
519 concentrations were standardised, i.e. divided by the initial concentration of the element in the
520 material. Figure 10a shows the evolution of standardised calcium concentration in the leaching
521 solutions as a function of time. To evaluate the dependence between the leaching of Ca and the acid
522 production of acidophilic SOB, the leaching of Ca is also represented as a function of sulfate produced
523 in Figure 10 b (as a reminder, there is a stoichiometric relationship between acid and sulfate
524 produced).

525

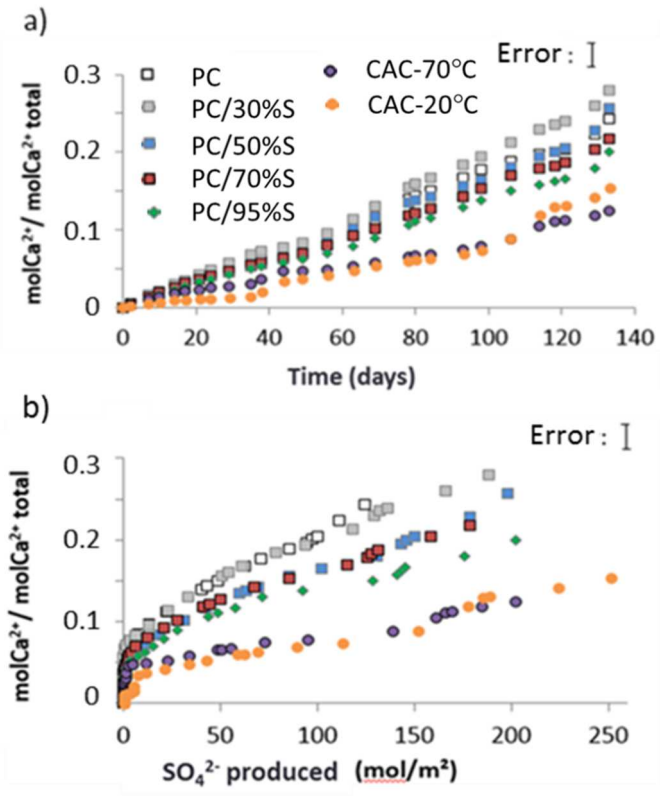

526

527 **Figure 10. Evolution of calcium concentration in the leaching solution divided by the initial calcium concentration**
528 **in the material as a function of a) time b) sulfate concentration in the leaching solution.**

529

530 Figure 10a shows that CAC binders released less Ca^{2+} than PC binders (relatively to their initial
531 composition of calcium). The difference between CAC and PC-based binders increased significantly
532 from 60 days, corresponding to the end of the pH fall to around 3.5 for all materials.

533 For all materials, the evolution of the calcium concentration in the leaching solution was a linear
534 function of time on the whole, even before the pH drop. Therefore diffusion limitation phenomena
535 may not have occurred over the entire test duration. Figure 11b shows that the normalised calcium
536 concentration represented as a function of the sulfate concentration was also linear, i.e. the calcium
537 concentration released by the material was linearly dependant on the amount of acid produced by SOB
538 (except for very low concentrations of sulfate, i.e. < 10 mol/m^2). With increasing GGBS content, the
539 normalised calcium concentration in the leaching solution decreased. For a similar acid attack strength,
540 there was no significant difference between the leaching of CAC-70°C and CAC-20°C, i.e. no
541 influence of conversion phenomena, in the conditions of the test.

Figure 11 shows the evolution of standardised aluminium concentration (i.e. divided by the initial aluminium concentration in the material) in the leaching solution as a function of time (a) and sulfate concentration (b), in order to compare leaching for a similar attack strength.

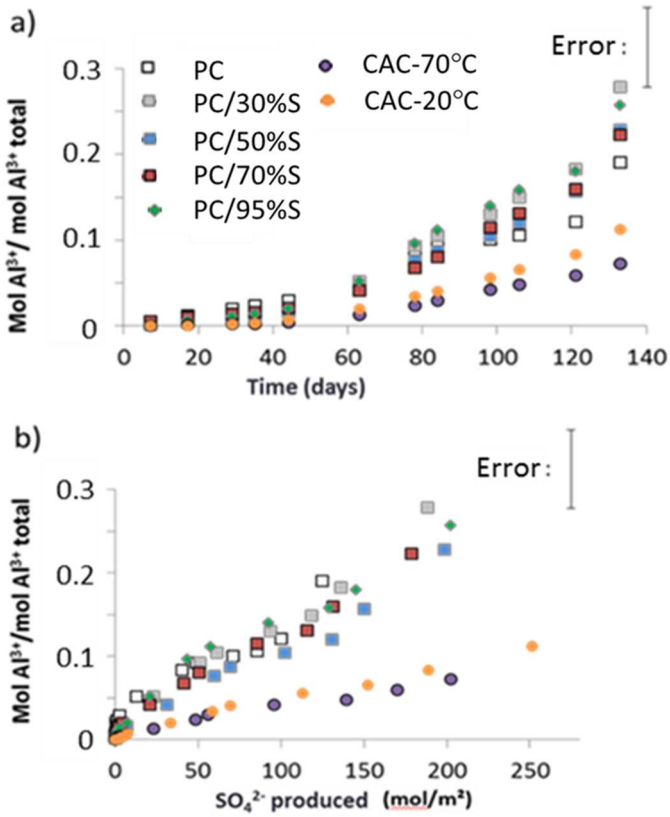

Figure 11. Evolution of aluminium concentration in the leaching solution divided by the initial aluminium concentration in the material as a function of a) time b) sulfate concentration in the leaching solution.

CAC-based material released relatively less aluminium than PC-based materials. Whatever the material composition, aluminium leaching increased significantly after 60 days, corresponding to low pH conditions. Figure 11 a shows that standardised aluminium leaching was higher for PC-based materials than for CAC systems. Figure 11 b shows that, for a similar attack, nearly 4 times less aluminium was leached from CAC-based materials than PC-based materials. Part of the aluminium contained in CAC phases was not released, probably because of the precipitation of AH_3 as a deterioration product. There was no significant difference between CAC-70°C and CAC-20°C, i.e.,

again, no influence of the conversion was detected in the conditions of the test. In addition, no significant difference can be observed whatever the substitution of PC-based materials (with higher relative errors compared to the calcium measured previously, due to lower concentrations).

3.3.2 Characterisation of cement pastes exposed to the BAC test

The SEM images of polished cross sections of PC, PC/70%S and CAC-70°C are presented, with a scheme of the image observations, in Figure 12. The inoculated surface is facing upward.

The deterioration zone started only at around 1 mm from the left hand side of the image due to the presence of a protective epoxy resin, which was initially deposited in order to have a reference for measuring depth of deterioration. The deteriorated area corresponded to the trickling zone where the leaching solution flowed. It can be seen that the deteriorated surfaces of the samples were relatively smooth. Because of the preparation protocol for SEM analyses, some pieces of the non-cohesive deteriorated zone were detached and are visible above the specimen in the theoretical dissolved zone (in black).

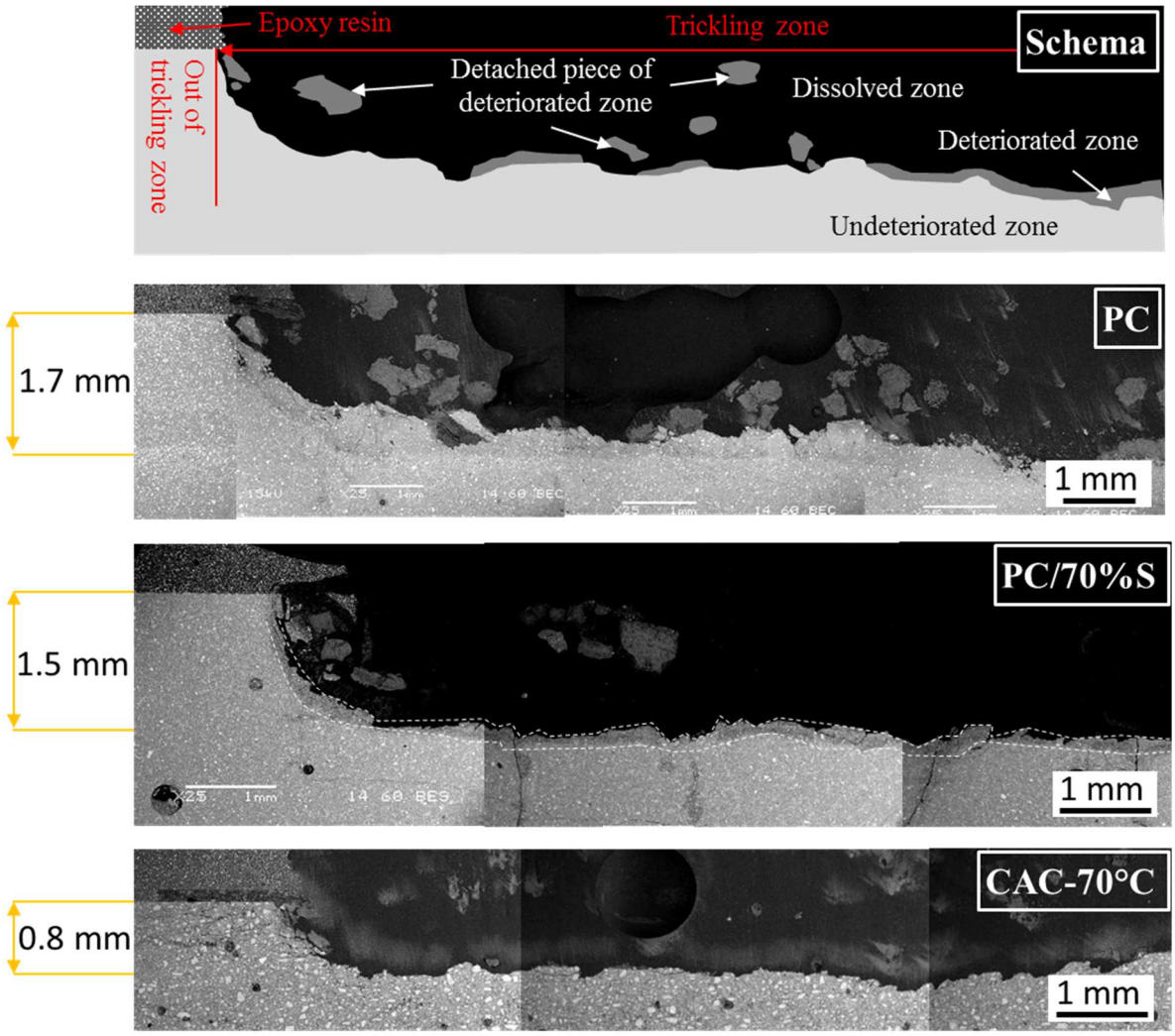

573

574 **Figure 12. Scheme and SEM-BSE image of cross section of deteriorated PC, PC/70%S and CAC-70°C cement**
575 **paste after 133 days in the BAC test.**

576

577 Figure 12 shows that a part of the cement pastes was dissolved. The upper surface in contact with the
578 biofilm appeared with dark grey contrast, meaning a lower density. EDS analyses on this zone showed
579 that it was almost totally decalcified and mainly composed of Al and Si for PC systems, and of Al for
580 CAC matrices (data not shown). This zone was thin, probably because (i) it was almost totally
581 dissolved by the acid, and (ii) it was fragile and thus removed during sample preparation. The
582 deteriorated layer thickness of CAC-based material (0.8 mm) was about half that of pure PC-based
583 materials (1.7 mm). The addition of 70% of GGBS led to a slightly smaller depth of deterioration (1.5

mm) than pure PC matrix. Some cracks perpendicular to the surface could be observed for the PC/70%S sample, and for other high GGBS content systems (data not shown).

XRD analyses were also carried out for the different samples: 1) on the top of the deteriorated surface, 2) a few hundred micrometres below the top surface and 3) in the sound area of the sample (1.5 cm deep). Reference specimens were also analysed. Figure 13 shows an illustration of XRD analysis for the PC/30%S specimen. The core and the reference specimens showed the same diffractograms. CH, hydrotalcite, and ettringite phases were logically identified in the core of the samples on the 0-24° range. In the intermediary zone, located a few hundred microns below the surface, ettringite and gypsum were detected, as were small quantities of CH. The diffractogram of the surface showed several halos, indicating an essentially amorphous nature of the microstructure, i.e. a gel (made of Si and Al, if we consider the results of EDS analyses), and some peaks of elemental sulfur, which is a product of the microbial reduction of $S_4O_6^{2-}$ in anaerobic conditions in the biofilm.

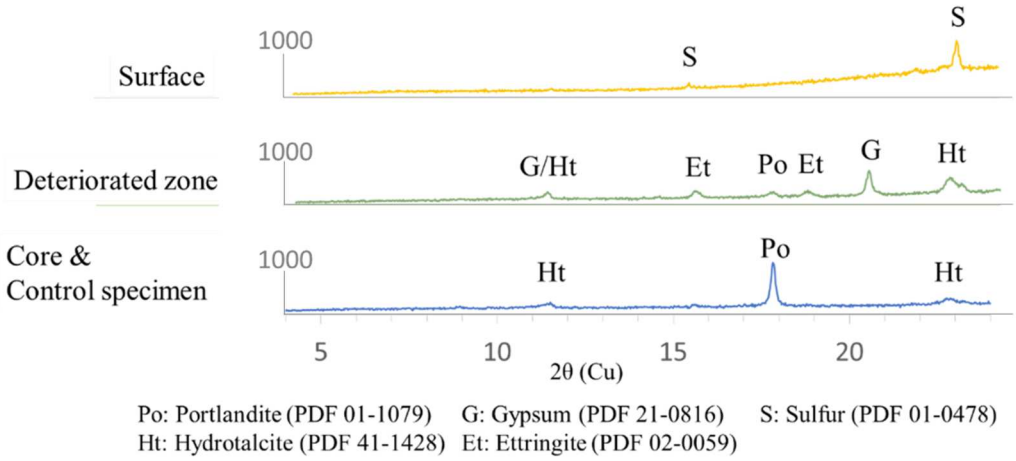

Figure 13. XRD analysis on massive sample of PC/30%S cement paste on the surface, in an intermediate zone (a few hundred microns below the surface) and in the core of the sample, as well as the control specimen.

Figure 14 shows XRD analysis of CAC-70°C in the same three different areas.

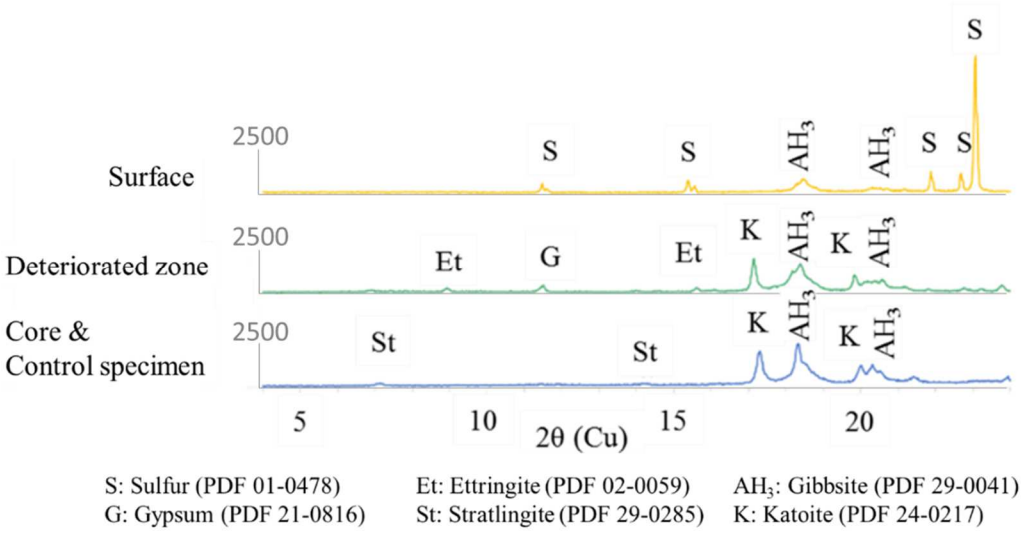

602

603 **Figure 14. XRD analysis on massive sample of CAC-70°C on the surface, in the deteriorated zone, in the core of**
604 **the sample, as well as the control specimen.**

605 The core and the reference specimens showed the same diffractograms, comprising typical phases of a
606 converted hydrated CAC: stratlingite, katoite and AH_3. In the intermediary deteriorated zone, gypsum
607 and ettringite were found. The surface was composed of elemental sulfur and AH_3. The presence of
608 elemental sulfur was due to the anaerobic biological and/or chemical reduction of tetrathionate in the
609 biofilm zone.

610

611 ## 4. Discussion

612

613 ### 4.1 Biological resistance

614

615 #### 4.1.1 Influence of soluble aluminium on SOB

616

617 Investigation of the inhibitory effect of Al^{3+} on SOB biofilms carried out in a reactor showed a
618 temporary inhibition of the maximal growth rate μ_{max} coupled with an increase of the oxidation yield
619 with the first injection of $AlCl_3$ up to 50 mM. The oxidation yield highlights the energy needed for
620 bacteria to survive in their environment (it increases when bacteria need to move, balance their inner

621 pressure, etc.). The modification of the environment of the bacteria implied that they had to adapt to
622 new conditions. The addition of $AlCl_3$ changed the ionic strength of the liquid, and thus induced an
623 osmotic stress which temporally decreased the bacterial activity [43]. The acclimation of SOB to the
624 new environment required energy and time. During the acclimation period (t1+24 hours) the bacterial
625 yield increased, revealing the overconsumption of oxygen. More energy was temporarily used for the
626 maintenance processes, i.e. to survive. But, at the end of this period, the maximal specific growth rate
627 was in the same range as before the addition of soluble aluminium; i.e. SOB bacteria developed a
628 resistance to the $AlCl_3$ environment. For the second addition up to Al^{3+}=~100 mM, the SOB growth
629 was not significantly impacted. The oxidation yield increased temporarily. A complementary study
630 showed that NaCl also induced a decrease in the bacterial growth of SOB. The effect on the maximal
631 specific growth rate recorded just after the addition may be attributed to the sudden modification of the
632 ionic pressure, inducing osmotic stress. The effect of aluminium could be a secondary parameter to
633 explain the temporary modification of μ_{max} after the first addition of $AlCl_3$.

634

635 Bacteria developed at pH 2 were less affected by the addition of $AlCl_3$; they were probably already
636 adapted to a concentrated ion environment due to the low pH during the selection of microorganisms.
637 Similar phenomena explained the lower influence of the aluminium injection on SOB developed on
638 CAC material, which was aluminium rich and released a high ion concentration when exposed to the
639 BAC test (Figure 6). Microorganisms in biofilms developed in inert conditions at pH 4 were more
640 impacted by the 50 mM $AlCl_3$ addition in the very short term, but their behaviour was equivalent to
641 that of microorganisms grown in other conditions 24h after the injection and then for the 100 mM
642 injection.

643

644 In a sewer network, pipes have a lifespan of 50 years, which gives bacteria plenty of time to adapt to
645 their environment. In such an environment, it is likely that, after their acclimation, they are little
646 affected by aluminium. In the light of these results, it may be concluded that the better resistance of

CAC mortar in aggressive conditions comparable to those implemented in this study may not be due to the inhibition of the SOB activity caused by the release of soluble aluminium in the aqueous phase.

4.1.2 Influence of material composition on SOB development

Even if free Al^{3+} was not responsible for the SOB inhibition, the solid material itself may have an influence on the sulfur-oxidising activity development or the biofilm composition. The better resistance of CAC might be due to a bacteriostatic effect related to the physicochemical parameters of the material [12,26]. In this study, the role of the chemistry and the mineralogy of the material were mainly considered but other parameters may have an influence on the colonisation of the material by microorganisms, such as the surface roughness, the surface tension, and the type of porosity (modifying the attachment of the microorganisms to the material).

The biogenic acid attack of the cementitious material induced a decrease of the pH in the solution trickling onto the surface. The pH evolution of the leaching solution showed a delayed acidification which depended on the material composition (Figure 7). One of the first reactions induced by the presence of acid on the surface of the material was the decalcification of calcic hydrates (CH, C-A-S-H, C_3AH_6 and CAH_{10} and anhydrous), and their release of OH^-. Figure 15 gives a comparison between the delay before biogenic acidification and PiOH, the intermediate hydroxide potential, as defined in 2.2.2.

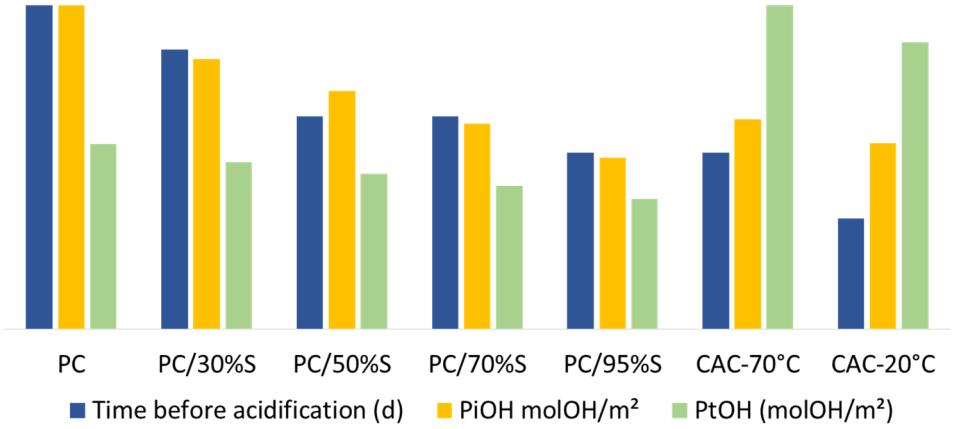

667

668 **Figure 15. PiOH, PtOH and the delay before biogenic acidification for each material tested**

669

670 Figure 15 shows the correlation between PiOH, PtOH and the time before biogenic acidification for
671 each material. The lower PiOH of CAC explains the earlier decrease of pH for this material compared
672 to PC. The increasing GGBS substitution level with PC also lowers the PiOH and the time before
673 acidification. There is no clear correlation between PtOH, the total potential in OH^- and the steps of
674 acidification.

675 At the early stage of acidification, production of sulfuric acid was low because of the small amount of
676 NSOB in the inoculum, the unfavourable growth conditions for ASOB and the low production of
677 sulfuric acid by NSOB compared to ASOB [2]. So, when an inoculation introduced few neutrophilic
678 bacteria, the buffer potential of the material had a significant influence on microbial development.
679 Elsewhere, the delay before acidification induced a delay before the ASOB development and therefore
680 in sulfuric acid production. CAC-based materials underwent earlier acidification, so the biogenic
681 sulfuric acid flow seen by these systems was higher. The conditions of aggressiveness were then
682 higher during the beginning of the experiment for CAC materials than for PC systems.

683 The analyses of the bacterial population revealed that there was a selection of similar populations on
684 each material tested, with predominance of ASOB and a minor proportion of NSOB. The composition
685 of the material did not induce the selection of a specific population depending on the nature of the

686 binder. The predominant bacterium at the end of the experiment was *Acidithiobacillus thiooxidans.*
687 The bacteria observed have already been mentioned in different studies of the literature as the
688 predominant species responsible for sulfuric acid production in the range of pH from ~4 to ~1 in sewer
689 networks [2,3,13]. It can also be mentioned that no *Acidithiobacillus ferrooxidans* has been observed.
690 This may be explained by bacterial growth conditions which were not suitable to such species,
691 especially with the use of white PC with low iron content. *Ac. ferrooxidans* has been reported in the
692 depth of concrete in an iron-rich front [44]. The biofilms analysed developed on the surface of the
693 material. It should be underlined that the bacterial population analyses were not quantitatively
694 absolute, and just informed on the relative proportions of microorganisms. However, the relatively
695 similar production of sulfate on each material (delayed or not) showed that the sulfur-oxidising
696 activity was not affected by the nature of the material.

697 Microscopic observation of the biofilms confirmed the development of microorganisms on the surface
698 of each material whatever its composition. Bacillus was observed on the surface of the materials but
699 was probably distributed throughout the volume of the biofilm before its dehydration. The sulfur-
700 oxidising species reported on cementitious material in sewer networks with such morphology were
701 generally *Acidithiobaccilus* or *Thiobaccilus* [13,45,46]. Filaments of ~1 µm diameter may correspond
702 to filamentous bacteria or exopolysaccharide (biopolymer produced by the bacteria for the
703 structuration of the biofilm). Filaments of diameter >3µm indicated probable presence of fungi. There
704 was no evidence of the material composition having a bacteriostatic effect on the development of
705 biofilms. However, it is notably that the experimental setup was operated in optimal conditions for
706 culture of SOB (continuously water, nutrients and sulfur susbtrate).

707 In this study, the only detected effect of the material on the biology was the influence of the PiOH on
708 the delay before acidification. This effect was responsible for a lower impact of CAC-based materials
709 (and higher PC-GGBS substitution) on the sulfate and thus acid production by SOB. CAC materials
710 were exposed to highly acid conditions earlier but exhibited more resistance to deterioration The
711 study of the biological activity also showed that there was no significant effect of materials rich in
712 aluminium on the SOB settlement activity or SOB selection using the BAC test, in contrast with the

713 literature hypothesis put forward in [17,26,29]. Moreover, the neutralisation capacity, corresponding to
714 the PtOH in this study, did not induce a lower sulfuric acid production by microorganisms on CAC
715 materials, as may have been previously assumed [12].

716

717 **4.2 Chemical resistance**

718

719 The better resistance of CAC binders could be mainly related to intrinsic physicochemical
720 characteristics (nature of the phases, reactivity, porosity, etc.) of the materials rather than a
721 bacteriostatic effect.

722 The biodeterioration phenomenology observed in cement matrices using the BAC test was globally in
723 accordance with in situ and laboratory data from the literature. The use of tetrathionate as reduced
724 sulfur substrate in the feeding solution allowed the selection of sulfur-oxidising activity [23,24].
725 Neutrophilic and then acidophilic SOBs were successively selected. The microbial activity induced the
726 production of sulfuric acid, which decreased the surface pH to about 2.5. The presence of elemental
727 sulfur was an indicator of the succession of oxidising reactions occurring from the tetrathionate
728 consumed by SOBs. The biogenic acid attack induced the decalcification and dissolution of the main
729 cementitious phases and the formation of a deteriorated zone that was rich in silicon and mainly
730 amorphous for PC systems, and rich in aluminium (AH_3 type) for CAC materials.

731 In the current study, sulfur based phases were precipitated in the deteriorated areas. Literature data
732 confirmed the presence of gypsum and ettringite in concrete deteriorated layers [15,25]. Calcium ions
733 released from dissolved calcic phases (C-A-S-H, CH, carbonates, C_3AH_6, etc.) diffused and reacted
734 with sulfate ions from sulfuric acid to form gypsum in oversaturation conditions relative to this phase.
735 A thick layer of calcium sulfate phases (gypsum, bassanite and anhydrite) was sometimes observed
736 during experimental campaigns on site [17,23,47]. Only a small quantity of gypsum and no basanite
737 nor anhydrite was observed in the present study. The aggressive nature of the BAC test, which was
738 designed for accelerated testing, may explain the lack of massive precipitation of calcium sulfate, due

739 to the very low pH conditions. Moreover, the wet-dry cycles, temperature, humidity, or hydraulicity
740 present in sewer conditions may play an important role in the precipitation of calcium sulfate phases
741 [3]. Wet-dry cycles induce a higher precipitation of such phases but also cause regular interruption of
742 the biological activity.

743 Different hydrates (AFm, C-A-S-H, ettringite, hydrotalcite) may be a source of aluminium for the
744 precipitation of ettringite. Reaction between gypsum and aluminate phases present in the system
745 induced the formation of ettringite in oversaturated solutions (rich in Al, SO_4 and Ca). Additionally,
746 some anhydrous phases (residual GGBS grains, C_2AS, etc.) could release aluminium even though their
747 contribution is not well identified in the literature. Ettringite was not always detected in experimental
748 campaigns of the literature and was generally localised near the sound area, due to its high solubility at
749 pH lower than 10.7 [22,24,26,47]. The formation of this expansive phase may lead to microcracking
750 phenomena with high crystallisation pressure. Some positive effects on porosity filling are not
751 documented in the field of biodeterioration.

752 The deterioration zone seemed to be more porous than the sound one, with darker shades on SEM
753 observations. The thickness of the deteriorated area was low and may be related to the high
754 aggressiveness of the BAC test caused by the low pH and the constant rinsing of the material surface,
755 inhibiting the oversaturation of the pore fluids. The biodeterioration mechanisms have been simulated
756 by comparing ion equilibrium. They explain the precipitation of the different phases and will be
757 presented in a further publication.

758 The total depth of deterioration was smaller for CAC-based materials than for PC-based materials.
759 [15,17,25]. This is in accordance with data obtained in laboratory and in situ conditions [17], [26].
760 Figure 16 shows that the depth of deterioration was strongly correlated to the standardised
761 concentration of calcium in leaching solution (i.e. divided by the initial concentration in the material).
762 This comparison showed the ability of leaching solution analyses to identify the intensity of the
763 biodeterioration and thus their possible use as a tool to compare different types of binders.

764 A hypothesis to explain the better resistance of CAC-based material is the lower reactivity of the
765 initial and decalcified phases [27,28]. With increasing GGBS content in PC-based material, the
766 standardised calcium leaching decreased. CAC-based materials underwent significantly lower
767 aluminium and calcium leaching than PC-based materials (Figure 10 and Figure 11). The theoretical
768 dissolution constants of the hydrated phases of the PC-based materials are lower than those of CAC-
769 based ones [48]. So, the dissolution of katoite (C_3AH_6) would be slower than that of common phases
770 in PC systems like CH. The AH_3 phase seemed to be intermixed with C_3AH_6 in the degraded area as
771 shown in Figure 12. The lower total content of calcic hydrates in PC-GGBS systems (due to the high
772 proportion of residual anhydrous GGBS grains) influenced this resistance. Anhydrous phases may be
773 less reactive to acid attack than hydrated phases [49,50]. In biodeteriorated zones of mortar pipe
774 sections exposed to the BAC test, Peyre Lavigne et al. observed an area where the hydrated paste was
775 dissolved but the anhydrous phases were preserved [25]. CAC-based materials presented a lower
776 standardised Al^{3+} leaching than PC-based systems, which meant that aluminium was more stable in
777 CAC systems. AH_3 phases are known to be stable over a wide pH range (pH ~ 4 to ~10 depending on
778 the aluminium concentration) [26,51]. In addition, no difference related to thermal curing of CAC-
779 based materials was observed: CAC-20°C and CAC-70°C showed equivalent Ca and Al leaching. The
780 presence of katoite (C_3AH_6) or CAH_{10} was not a determining parameter for the resistance of CAC
781 binders in the very aggressive conditions developed in the BAC test.

782 In the literature, the lower diffusion properties of CAC phases are assumed to account for the better
783 resistance of these binders [15,26–28]. Figure 16 compares the deterioration parameters (depth of
784 deterioration, standardised calcium leached) and initial water intrusion porosity for the different
785 systems.

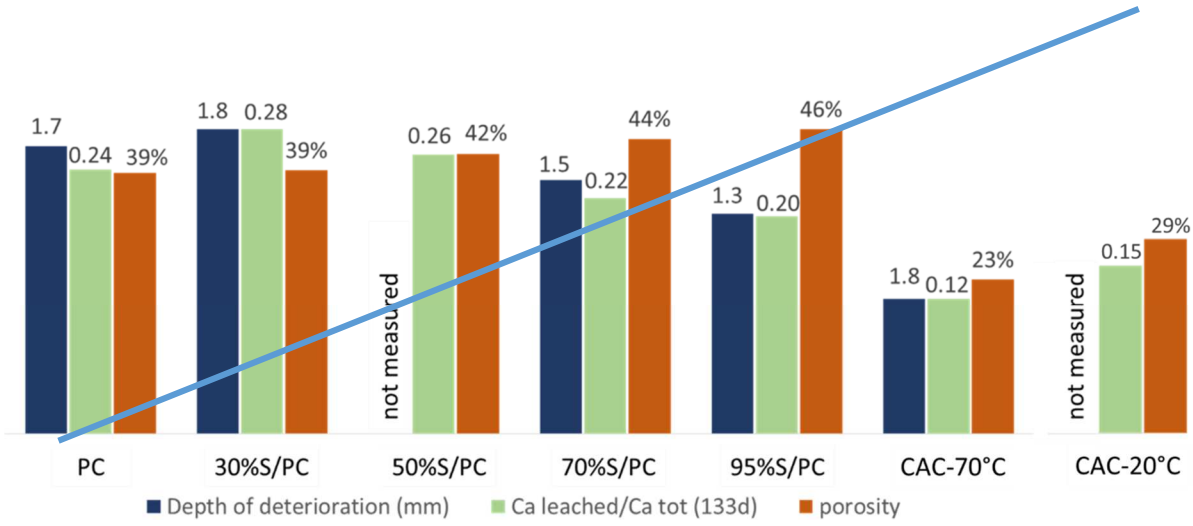

Figure 16. Comparison between depth of deterioration, calcium leaching and initial water porosity for PC, PC/30%S, PC/50%S, PC/70%S, PC/95%S and CAC-70°C.

With increasing GGBS content in PC-based material, the initial porosity increased slightly [52]. This effect has often been reported in the literature but was generally combined with a refinement of porosity limiting the diffusion process. CAC-based material had the lowest initial porosity. This was partly due to the initial lower water/solid ratio (0.3 against 0.4 for PC-based materials). No correlation between the initial total water porosity and the leaching of the cementitious matrix can be evidenced on the series of OPC-slag based materials (Ca leaching and depth of deterioration tend to decrease while the initial matrix porosity increases in higher slag content mixes), which would indicate that initial porosity was not a critical characteristic in the biodeterioration of materials in such aggressive conditions. For CAC-based materials, the difference in phase composition and in porosity may influence the calcium leaching. Moreover, as it can be seen in Figure 8, CAC 20°C specimens were exposed to a higher sulfate flow due to the earlier biogenic acidification (Figure 7). The biogenic acid attack induced the formation of deteriorated areas, possibly with different diffusion properties. These deteriorated areas may have had a positive effect by limiting both the diffusion of aggressive ions inside the matrix and leaching of calcium outside the cementitious binder. To understand the influence of the porosity in such conditions, the biodeterioration of a theoretical CAC material with initial

806 porosity similar to that of PC but having the same composition as CAC-70°C has been simulated and
807 will be the subject of a further publication.

808

809 In conclusion, the reactivity of the phases is likely to control the dissolution of the cement matrix and
810 thus the resistance of the materials submitted to the BAC test in aggressive conditions. Diffusion
811 properties were probably a secondary parameter accounting for the deterioration process kinetics in the
812 aggressive conditions of this study. The difference of chemical resistance between the cementitious
813 phases and their associated diffusion properties has been simulated using a biodeterioration model
814 combining biological activity and dissolution/precipitation of solid phases and will be presented in a
815 further publication.

816

817 **5. Conclusion**

818

819 The present paper studied the reliability of the main hypotheses found in the literature to explain the
820 better resistance of CAC-based material than PC systems in a sewer network. The absence of a long-
821 term bacteriostatic effect of soluble aluminium up to 100 mM (from $AlCl_3$) on SOB activity was
822 demonstrated using controlled batch reactors bacterial consortia selected in different conditions.

823 Matrices with a wide range of aluminium contents and different phase assemblages were considered.
824 They were based on PC with different GGBS substitution levels (from 0 to 95 wt.%) and CAC. The
825 cement pastes were exposed to an accelerated laboratory biodeterioration test (BAC test) for 133 days
826 with final pH of 2.5 to simulate sewer conditions. It was shown that the intermediate hydroxide
827 potential (i.e. the quantity of hydroxide ions released by the dissolution of calcic phases) was
828 correlated with the beginning of strong acidification and so the start of the activity of ASOBs. More
829 aggressive conditions (due to an earlier acidification) were obtained for CAC systems and, to a lower
830 extent, for PC-GGBS systems with high slag replacement levels. However, these materials were more
831 resistant to biodeterioration than PC systems. Moreover, no difference in population selection or

characteristics of the biofilm was evidenced between the different materials. There was also no evidence of a bacteriostatic effect of aluminium rich materials on the SOB activity.

The better resistance of CAC-based materials compared to PC-based was verified by SEM observations The leaching of sulfate, calcium and aluminium produced during the biodeterioration test were consistent with the SEM observations, which demonstrated the ability of leaching analysis to monitor the kinetics of biodeterioration. The phenomenology of deterioration was consistent with the literature. Calcic phases were dissolved whereas deteriorated areas rich in silica, for PC-based systems, and rich in aluminium, for CAC systems, were formed. The thicknesses of these areas were reduced due to the high aggressiveness of the deterioration test, which led to dissolution of the surface material. Moreover sulfur based products were precipitated in the upper part of the sample in contact with the biofilm. The resistance to biodeterioration of CAC systems was linked to physicochemical characteristics of the material when faced with biogenic attack. The transport phenomena limiting the dissolution of the cement matrix seemed to constitute a secondary process in the conditions of the BAC test. The phase stability of initial and secondary precipitated phases was probably the key parameter explaining the better resistance of CAC-based material and PC-GGBS compared to PC binders in sewer network conditions. To confirm and improve the understanding of deterioration mechanisms, a simulation has been performed using a model taking account of the biological activity (only influenced by the PiOH) of the different populations of SOBs and the physicochemical evolutions of the material (leaching solution composition, dissolution/precipitation of phases, evolution of porosity and diffusion properties) and will be presented in a further publication.

Acknowledgments

This work was funded by the Research Centre of Saint-Gobain Pont-à-Mousson. The authors also would like to thank Institut Universitaire de France (Research grant of A. Bertron, junior member 2016-2021) for complementary funding. The authors gratefully acknowledge the technical staff for the experimental set up and help in the analyses: Evrard Mengel, Maud Shiettekatte, Vanessa Mazars, and

Guillaume Lambare. The authors also thank Myriam Mercade and Marie-Line de Solan Bethmale for their assistance in the biofilm observation, and all those who helped in the achievement of this project.

References

[1] T. Mori, M. Koga, Y. Hikosaka, T. Nonaka, F. Mishina, Y. Sakai, J. Koizumi, Microbial Corrosion of Concrete Sewer Pipes, H2S Production from Sediments and Determination of Corrosion Rate, Water Sci. Technol. 23 (1991) 1275–1282. doi:10.2166/wst.1991.0579.

[2] D.J. Roberts, D. Nica, G. Zuo, J.L. Davis, Quantifying microbially induced deterioration of concrete: initial studies, Int. Biodeterior. Biodegradation. 49 (2002) 227–234. doi:10.1016/S0964-8305(02)00049-5.

[3] C. Grengg, F. Mittermayr, A. Baldermann, M.E. Böttcher, A. Leis, G. Koraimann, P. Grunert, M. Dietzel, Microbiologically induced concrete corrosion: A case study from a combined sewer network, Cem Concr Res. 77 (2015) 16–25. doi:10.1016/j.cemconres.2015.06.011.

[4] H. Jensen, Hydrogen sulfide induced concrete corrosion of sewer networks; Section of Environmental Engineering, Aalborg University, (2009). http://vbn.aau.dk/files/19097739/henriette_stokbro-ph.d.pdf.

[5] M. O'Connell, C. McNally, M.G. Richardson, Biochemical attack on concrete in wastewater applications: A state of the art review, Cem Concr Compos. 32 (2010) 479–485. doi:10.1016/j.cemconcomp.2010.05.001.

[6] S. Mortezania, F. Othman, Cost analysis of pipes for application in sewage systems, Mater Des. 33 (2012) 356–361. doi:10.1016/j.matdes.2011.01.062.

[7] A.G. Boon, Septicity in sewers: Causes, consequences and containment, Water Sci. Technol. 31 (1995) 237–253. doi:10.1016/0273-1223(95)00341-J.

[8] A.P. Joseph, J. Keller, H. Bustamante, P.L. Bond, Surface neutralization and H2S oxidation at early stages of sewer corrosion: Influence of temperature, relative humidity and H2S concentration, Water Res. 46 (2012) 4235–4245. doi:10.1016/j.watres.2012.05.011.

[9] R. Islander, J. Devinny, F. Mansfeld, A. Postyn, H. Shih, Microbial Ecology of Crown Corrosion in Sewers, J Environ Eng (New York). 117 (1991) 751–770. doi:10.1061/(ASCE)0733-9372(1991)117:6(751).

[10] T. Mori, T. Nonaka, K. Tazaki, M. Koga, Y. Hikosaka, S. Noda, Interactions of nutrients, moisture and pH on microbial corrosion of concrete sewer pipes, Water Res. 26 (1992) 29–37. doi:10.1016/0043-1354(92)90107-F.

[11] T. Wells, R.E. Melchers, Modelling concrete deterioration in sewers using theory and field observations, Cem Concr Res. 77 (2015) 82–96. doi:10.1016/j.cemconres.2015.07.003.

[12] A. Bielefeldt, M.G.D. Gutierrez-Padilla, S. Ovtchinnikov, J. Silverstein, M. Hernandez, Bacterial Kinetics of Sulfur Oxidizing Bacteria and Their Biodeterioration Rates of Concrete Sewer Pipe Samples, J Environ Eng (New York). 136 (2010) 731–738. doi:10.1061/(ASCE)EE.1943-7870.0000215.

[13] S. Okabe, M. Odagiri, T. Ito, H. Satoh, Succession of Sulfur-Oxidizing Bacteria in the Microbial Community on Corroding Concrete in Sewer Systems, Appl Environ Microbiol. 73 (2007) 971–980. doi:10.1128/AEM.02054-06.

[14] C. Grengg, F. Mittermayr, G. Koraimann, F. Konrad, M. Szabó, A. Demeny, M. Dietzel, The decisive role of acidophilic bacteria in concrete sewer networks: A new model for fast progressing microbial concrete corrosion, Cem Concr Res. 101 (2017) 93–101. doi:10.1016/j.cemconres.2017.08.020.

[15] M.W. Kiliswa, Composition and microstructure of concrete mixtures subjected to biogenic acid corrosion and their role in corrosion prediction of concrete outfall sewers, PhD Thesis, University of Cape Town, 2016. https://open.uct.ac.za/handle/11427/20363.

907 [16] G. Renaudin, I/ Etude d'un hydroxyde simple d'aluminium : La bayerite II/ Etude d'une famille
908 d'hydroxydes doubles lamellaires d'aluminium et de calcium : les phases AFM (Aluminates
909 Tétracalciques Hydrates), Université Nancy 1, 1998. http://www.theses.fr/1998NAN10302.
910 [17] M.G. Alexander, C. Fourie, Performance of sewer pipe concrete mixtures with portland and
911 calcium aluminate cements subject to mineral and biogenic acid attack, Mater Struct. 44 (2011)
912 313–330. doi:10.1617/s11527-010-9629-1.
913 [18] J.L. Davis, D. Nica, K. Shields, D.J. Roberts, Analysis of concrete from corroded sewer pipe, Int
914 Biodeterior Biodegradation. 42 (1998) 75–84. doi:10.1016/S0964-8305(98)00049-3.
915 [19] S. Ehrich, L. Helard, R. Letourneux, J. Willocq, E. Bock, Biogenic and Chemical Sulfuric Acid
916 Corrosion of Mortars, J Mater Civ Eng. 11 (1999) 340–344. doi:10.1061/(ASCE)0899-
917 1561(1999)11:4(340).
918 [20] W. Sand, E. Bock, Biotest system for rapid evaluation of concrete resistance to sulfur-oxidizing
919 bacteria, Mater Perform. 26 (1987) 14–17.
920 [21] E. Vincke, S. Verstichel, J. Monteny, W. Verstraete, A new test procedure for biogenic sulfuric
921 acid corrosion of concrete, Biodegradation. 10 (1999) 421–428. doi:10.1023/A:1008309320957.
922 [22] N. De Belie, J. Monteny, A. Beeldens, E. Vincke, D. Van Gemert, W. Verstraete, Experimental
923 research and prediction of the effect of chemical and biogenic sulfuric acid on different types of
924 commercially produced concrete sewer pipes, Cem Concr Res. 34 (2004) 2223–2236.
925 doi:10.1016/j.cemconres.2004.02.015.
926 [23] M. Peyre Lavigne, A. Bertron, C. Patapy, X. Lefebvre, E. Paul, Accelerated test design for
927 biodeterioration of cementitious materials and products in sewer environments, Matériaux &
928 Techniques. 103 (2015). doi:10.1051/mattech/2015018.
929 [24] M. Peyre Lavigne, A. Bertron, L. Auer, G. Hernandez-Raquet, J.-N. Foussard, G. Escadeillas, A.
930 Cockx, E. Paul, An innovative approach to reproduce the biodeterioration of industrial
931 cementitious products in a sewer environment. Part I: Test design, Cem Concr Res. 73 (2015)
932 246–256. doi:10.1016/j.cemconres.2014.10.025.
933 [25] M. Peyre Lavigne, A. Bertron, C. Botanch, L. Auer, G. Hernandez-Raquet, A. Cockx, J.-N.
934 Foussard, G. Escadeillas, E. Paul, Innovative approach to simulating the biodeterioration of
935 industrial cementitious products in sewer environment. Part II: Validation on CAC and BFSC
936 linings, Cem Concr Res. 79 (2016) 409–418. doi:10.1016/j.cemconres.2015.10.002.
937 [26] J. Herisson, M. Guéguen-Minerbe, E.D. van Hullebusch, T. Chaussadent, Behaviour of different
938 cementitious material formulations in sewer networks, Water Sci Technol. 69 (2014) 1502–1508.
939 doi:10.2166/wst.2014.009.
940 [27] K.L. Scrivener, J.-L. Cabiron, R. Letourneux, High-performance concretes from calcium
941 aluminate cements, Cem Concr Res. 29 (1999) 1215–1223. doi:10.1016/S0008-8846(99)00103-
942 9.
943 [28] A. Grandclerc, Compréhension des mecanismes de biodétérioration des matériaux cimentaires
944 dans les reseaux d'assainissement : étude experimentale et modelisation, PhD Thesis, Université
945 Paris-Est, 2017. https://tel.archives-ouvertes.fr/tel-01685132/document.
946 [29] F. Saucier, S. Lamberet, Calcium aluminate concrete for sewers: going from qualitative to
947 quantitative evidence of performance, in: Alexander MG, Bertron A (Eds), Final Conference on
948 Concrete in Aggresive Aqueous Environments - Performance, Testing and Modeling.
949 Proceedings of the RILEM TC 211-PAE, Toulouse, France., 2009: pp. 398–407.
950 [30] H. Hornain, GranDuBé: grandeurs associées à la durabilité des bétons, Presses des Ponts, France,
951 2007.
952 [31] C. Yu, W. Sun, K. Scrivener, Degradation mechanism of slag blended mortars immersed in
953 sodium sulfate solution, Cem Concr Res. 72 (2015) 37–47.
954 doi:10.1016/j.cemconres.2015.02.015.
955 [32] M. Mouret, E. Ringot, A. Bascoul, Image analysis: a tool for the characterisation of hydration of
956 cement in concrete – metrological aspects of magnification on measurement, Cem Concr Res. 23
957 (2001) 201–206. doi:10.1016/S0958-9465(00)00061-5.
958 [33] V. Kocaba, E. Gallucci, K.L. Scrivener, Methods for determination of degree of reaction of slag
959 in blended cement pastes, Cem Concr Res. 42 (2012) 511–525.
960 doi:10.1016/j.cemconres.2011.11.010.

[34] C. Gosselin, Microstructural development of calcium aluminate cement based systems with and without supplementary cementitious materials, PhD thesis, EPFL (Lausanne), 2009.
[35] P. Hewlett, Lea's Chemistry of Cement and Concrete, Elsevier, 2003.
[36] A. Buvignier, Caractérisation du rôle de l'aluminium dans les interactions entre les microorganismes et les matériaux cimentaires dans le cadre des réseaux d'assainissement, PhD Thesis, INSA Toulouse - Université Fédérale Toulouse Midi-Pyrénée, 2018. https://tel.archives-ouvertes.fr/tel-01963228/document.
[37] R. Letourneux, K. Scrivener, The resistance of calcium aluminate cements to acid corrosion in wastewater applications, in: Ravindra K. Dhir, Thomas D. Dyer (Eds.), Modern Concrete Materials: Binders, Additions and Admixtures, Dundee, 2009: pp. 275–283. doi:10.1680/mcmbaaa.28227.0028.
[38] Spérandio, Paul, Estimation of wastewater biodegradable COD fractions by combining respirometric experiments in various So/Xo ratios, Water Res. 34 (2000) 1233–1246. doi:10.1016/S0043-1354(99)00241-9.
[39] A. Buvignier, M. Peyre Lavigne, O. Robin, M. Bounouba, C. Patapy, A. Bertron, E. Paul, Influence of dissolved aluminum concentration on sulfur-oxidizing bacterial activity in the biodeterioration of concrete, Applied and Environmental Microbiology. Accepted for publication (2019).
[40] A. Bertron, G. Escadeillas, P. de Parseval, J. Duchesne, Processing of electron microprobe data from the analysis of altered cementitious materials, Cem Concr Res. 39 (2009) 929–935. doi:10.1016/j.cemconres.2009.06.011.
[41] A. Bertron, J. Duchesne, G. Escadeillas, Accelerated tests of hardened cement pastes alteration by organic acids: analysis of the pH effect, Cem Concr Res. 35 (2005) 155–166. doi:10.1016/j.cemconres.2004.09.009.
[42] R.B. Martin, The chemistry of aluminum as related to biology and medicine, Clin Chem. (1986) 1797–1806.
[43] R.D. Sleator, C. Hill, Bacterial osmoadaptation: the role of osmolytes in bacterial stress and virulence, FEMS Microbiol Rev. 26 (2002) 49–71. doi:10.1111/j.1574-6976.2002.tb00598.x.
[44] C. Grengg, F. Mittermayr, N. Ukrainczyk, G. Koraimann, S. Kienesberger, M. Dietzel, Advances in concrete materials for sewer systems affected by microbial induced concrete corrosion: A review, Water Res. 134 (2018) 341–352. doi:10.1016/j.watres.2018.01.043.
[45] K. Milde, W. Sand, W. Wolff, E. Bock, Thiobacilli of the Corroded Concrete Walls of the Hamburg Sewer System, Microbiology. 129 (1983) 1327–1333. doi:10.1099/00221287-129-5-1327.
[46] H. Satoh, M. Odagiri, T. Ito, S. Okabe, Microbial community structures and in situ sulfate-reducing and sulfur-oxidizing activities in biofilms developed on mortar specimens in a corroded sewer system, Water Res. 43 (2009) 4729–4739. doi:10.1016/j.watres.2009.07.035.
[47] A. Grandclerc, M. Guéguen-Minerbe, I. Nour, P. Dangla, T. Chaussadent, Impact of cement composition on the adsorption of hydrogen sulphide and its subsequent oxidation onto cementitious material surfaces, Constr Build Mater. 152 (2017) 576–586. doi:10.1016/j.conbuildmat.2017.07.003.
[48] L. De Windt, P. Devillers, Modeling the degradation of Portland cement pastes by biogenic organic acids, Cem Concr Res. 40 (2010) 1165–1174.
[49] O. Oueslati, J. Duchesne, Resistance of blended cement pastes subjected to organic acids: Quantification of anhydrous and hydrated phases, Cem Concr Compos. 45 (2014) 89–101. doi:10.1016/j.cemconcomp.2013.09.007.
[50] A. Bertron, J. Duchesne, G. Escadeillas, Degradation of cement pastes by organic acids, Mater Struct. 40 (2007) 341–354. doi:10.1617/s11527-006-9110-3.
[51] S. Lamberet, D. Guinot, E. Lempereur, J. Talley, C. Alt, Field investigations of high performance calcium aluminate mortar for wastewater applications, in: Fentiman CH, Mangabhai RJ & Scrivener KL (Eds), Proceedings of the centenary Conference, Avignon, France, 2008: pp. 269–277.
[52] R.F. Feldman, Significance of Porosity Measurements on Blended Cement Performance, Special Publication. 79 (1983) 415–434. doi:10.14359/6705.